63-4-2

SIXTH QUARTERLY PROGRESS REPORT

HIGH TEMPERATURE THERMOELECTRIC RESEARCH

29 MARCH 1963 – 28 JUNE 1963

CONTRACT AF 33(657)-7387
PROJECT NO. 8173 TASK NO. 817302-9

AUTHOR

C. M. HENDERSON

CONTRIBUTORS
G. H. RINGROSE
R. G. AULT
EMIL BEAVER
R. J. JANOWIECKI
H. B. JANKOWSKY
L. REITSMA

MONSANTO RESEARCH CORPORATION
A SUBSIDIARY OF MONSANTO CHEMICAL COMPANY

DAYTON LABORATORY
DAYTON 7, OHIO

NOTICE

"The work covered by this report was accomplished under Air Force Contract AF 33(657)-7387 but this report is being published and distributed prior to Air Force review. The publication of this report, therefore, does not constitute approval by the Air Force of the findings or conclusions contained herein. It is published for the exchange and stimulation of ideas."

DISTRIBUTION LIST

Cys	ACTIVITIES AT WPAFB
2	ASAPR (Library)
1	ASRMA
6	ASRPP-20 (C. Glassburn)

OTHER DEPT. OF DEFENSE ACTIVITIES

Navy

1 Mr. Bernard B. Rosenbaum
Bureau of Ships (Code 342B)
Department of the Navy
Washington 25, D. C.

Air Force

1 SSD (SSTRE, Maj. Iller)
AF Unit Post Office
Los Angeles 45, Calif.

1 RADC (RASGP, Mr. P. Richards)
Griffiss AFB NY

25 ASTIA (TIPDR)
Arlington Hall Stn
Arlington 12, Va.

NON-GOVERNMENT INDIVIDUALS & ORGANIZATIONS

1 Aerospace Corporation
Attn: Library Technical Documents Group
P.O. Box 95085
Los Angeles 45, California

1 Jet Propulsion Laboratory
California Institute of Technology
Attn: Mr. Paul Goldsmith
4800 Oak Grove Drive
Pasadena, California

OTHER GOVERNMENT ACTIVITIES

1 U.S. Atomic Energy Commission
Office of Technical
Information Extension
Attn: M. L. Pflueger
P. O. Box 62
Oak Ridge, Tennessee

FOREWORD

This report describes work performed under Contract AF 33(657)-7387, Project No. 8173, Task No. 817302-9 during the period 29 March to 28 June 1963. The contract concerns development of a high temperature thermoelectric generator, and is under sponsorship of the Static Energy Conversion Branch, Flight Vehicle Power Division, AF Aero-Propulsion Laboratory, Wright-Patterson Air Force Base, Ohio. For the Air Force, Mr. Charles Glassburn is project engineer.

The contract is being performed by Monsanto Research Corporation at its Dayton Laboratory with C. M. Henderson as project leader. Working with him are R. G. Ault, Emil Beaver, H. B. Jankowsky, R. J. Janowiecki, L. Reitsma, and G. H. Ringrose. Technical assistance was provided by R. R. Hawley, C. D. Reinhardt and D. Sevy.

ABSTRACT

The experimental model generator, previously operated for 2556 hr at 1200°C in a vacuum of 10^{-5} - 10^{-6} mm Hg without degradation of power output, was disassembled and examined. No physical change or damage to its MCC 50-graphite thermoelements was found.

Formulations of new p- and n-type thermoelectric materials, to supplement MCC 50, were standardized and techniques developed for forming them into segmented thermoelements. Realistic measurements of segmented p- and n-type thermoelements showed that efficiences ranging from ~3% for p-type to ~6% for n-type can be attained for such units when operating between ~1200°C and ~460°C.

Emittance measurements on a new coating for use on the copper radiators of the advanced experimental model generator, or the surfaces of space vehicles, showed that it is capable of ϵ's ranging from ~0.9 at 500°C to ~0.98 at 900°C.

Progress in overcoming hot-pressing problems and flame-spraying techniques concerned with making segmented thermoelements is described and a detailed design for an advanced experimental model generator capable of a nominal 50 watts output at ~10 watt/lb ratio is presented.

ABSTRACT

The experimental model generator, previously operated for 2556 hr at 1200°C in a vacuum of 10^{-5} - 10^{-6} mm Hg without degradation of power output, was disassembled and examined. No physical change or damage to its MCC 50-graphite thermoelements was found.

Formulations of new p- and n-type thermoelectric materials, to supplement MCC 50, were standardized and techniques developed for forming them into segmented thermoelements. Realistic measurements of segmented p- and n-type thermoelements showed that efficiences ranging from ~3% for p-type to ~6% for n-type can be attained for such units when operating between ~1200°C and ~460°C.

Emittance measurements on a new coating for use on the copper radiators of the advanced experimental model generator, or the surfaces of space vehicles, showed that it is capable of ϵ's ranging from ~0.9 at 500°C to ~0.98 at 900°C.

Progress in overcoming hot-pressing problems and flame-spraying techniques concerned with making segmented thermoelements is described and a detailed design for an advanced experimental model generator capable of a nominal 50 watts output at ~10 watt/lb ratio is presented.

TABLE OF CONTENTS

LIST OF FIGURES

LIST OF FIGURES (Cont'd)

LIST OF FIGURES (Cont'd)

LIST OF FIGURES (Cont'd)

LIST OF FIGURES (Cont'd)

LIST OF TABLES

I. INTRODUCTION AND SUMMARY

A. BACKGROUND

The overall program objective is to conduct applied research to establish the technical feasibility of utilizing a high temperature thermoelectric generator with a nuclear heat source to produce a long-lived power supply for aerospace vehicles. This effort, the second phase of a program initiated 1 October 1961, is directed toward improving and further defining high-temperature thermoelectric generator components based on new high temperature (1200°C) thermoelectric materials originated by Monsanto Chemical Company (MCC). The results of this work are to be used to design and fabricate an advanced experimental model of nominal 50 watts output at about 6 volts and 10-20 watts/lb ratio in a space environment.

The status of research on each phase of the 1962-63 project is presented below:

Phase I - Experimental Model Evaluation The nominal 5-watt experimental generator, fabricated and preliminarily tested under the first year's contract, was subjected during the first two quarters of the 1962-62 project to a sustained performance evaluation of 2556 hr at a hot junction temperature (T_h) of 1200°C (+25°C - 4°C) in a vacuum of 10^{-5} to 10^{-6} mm Hg without degradation of its power producing characteristics. Power/weight ratios of 2.7 to 2.86 watts/lb, exclusive of heat source, were obtained for this generator of unoptimized design operating into an approximately matched electrical resistance load. No further testing of the experimental model generator was attempted this quarter.

To permit the design of the advanced model generator to benefit from the results of the 2500-hr test, the experimental model was disassembled and examined prior to completing the design of the advanced model. The results of this study are presented in this quarterly report.

Phase II - Component Improvement and Evaluation Effort on this phase was directed toward improving MCC 50 (a p-type material) and the following supplementary thermoelectric materials.

1. MCC 60 (n-type) for use to 1200°C.
2. MCC 40 (p-type) for use to about 900°C.
3. MCC 40 (n-type) for use to about 900°C.

Effort was also to be directed toward developing improved junction-forming techniques between the thermoelectric materials and the thermal and electrical contacts required for the advanced experimental model generator. Additionally, effort was to be directed toward developing hot-pressing techniques for producing segmented thermoelements of the most improved formulations of the four basic MCC thermoelectric materials.

Investigation of plasma and flame techniques for fabricating improved sandwich-type thermoelements and more efficient generators was also planned. Improved thermoelectric material formulations were to be evaluated in thermoelement form, with the best formulation for each of the four types of thermoelectric materials to be subjected in segmented thermoelement form to sustained evaluation test as a p-n module.

Phase III - Advanced Experimental Model The design of a nominal 50-watt generator, based on the results of the studies made in Phases I and II, was to be completed and to be presented in this quarterly report.

In the preceding quarterly reports, the word "module" was used to signify a multi-segment thermoelectric leg or arm of a p-n couple. Since "module" is frequently used by others to mean a p-n couple, or a multiple p-n couple arrangement, the word "thermoelement", meaning in this case a single thermoelectric leg or arm consisting of one or more thermoelectric materials with their terminal thermal and electrical contacts bonded together in layers (segments), is used in this quarterly, The term "module", as explained above, is used to denote an assembly of more than two thermoelements.

B. SUMMARY

Plans to voluntarily test the experimental model generator at 1300 °C and higher temperature, following completion of 2556-hr tests at 1200 °C were abandoned when it became necessary to use all test facilities in solving junction problems concerned with producing segmented thermoelements for the advanced experimental model generator. Disassembly and examination of the experimental model, prior to designing the advanced experimental model, confirmed an early hypothesis that the molybdenum-graphite hot-end contacts had been loosened by repeated inspection operations and by thermal expansions. Metal plating on the hot-end sections of the experimental model resulted from vaporization of the resistance heater and inner radiation shields, and doubtlessly reduced the power output of the generator prior to starting the 2556-hr test.

Formulations for the two p- and two n-type thermoelectric materials to be used in producing segmented thermoelements for the advanced experimental model generator were standardized and their properties measured. Measurements on individual p- and n-type segmented thermoelements, under conditions apt to be encountered by the advanced experimental model, showed that practical overall thermal efficiencies per thermoelement will range from ~3% for p-type to ~6% for n-type when the generator is operating between 1200°C and 460°C in a space environment.

Measurements on a new radiator coating material showed emittances ranging from 0.9 at ~500°C to 0.98 at ~900°C in a vacuum.

Design studies dictated changing from 0.5" dia. to 0.375" dia. thermoelements to permit attainment of ~10 watts/lb performance for the advanced experimental model. Hot-pressing problems initially limited yields of the segmented 0.375" dia. thermoelements to less than 10%, but metallographic examinations and hot-pressing studies finally resulted in 60-70% yields of usable thermoelements. Further progress was made in developing techniques for producing thermoelements by flame and plasma techniques -- as alternate and lower cost means of producing thermoelements.

Further sustained testing on p-n couples constructed from segmented thermoelements were run which indicate that power degradation with time should be quite low for the types of thermoelements to be used in the advanced experimental model generator. A 3-tier 24-thermoelement generator based on 0.5" dia. thermoelements was assembled and tested to investigate assembly, radiator, and durability aspects of design features contemplated for the advanced experimental model. Changes in radiator design resulted from this work.

A detailed design for the advanced experimental model generator was developed and is presented in this quarterly. On the basis of this design ~10 watts/lb should be attainable with the end-product generator.

II. RESEARCH AND DEVELOPMENT

A. PHASE I - EXPERIMENTAL MODEL EVALUATION

Plans to voluntarily study the effect of operating this generator at 1300°C and higher temperatures were postponed the first half of this quarter when it became necessary to convert its vacuum test facility to a unit for evaluating segmented p-n couples for use in the advanced experimental model generator. Later, difficulties in attaining reasonable fabrication yields of p- and n-type segmented thermoelements prevented use of the needed vacuum facility, so that it was necessary to abandon plans to test the experimental model generator at 1300°C. In order that knowledge gained from operation of this generator for 2500 hr be available for the design of the advanced experimental model generator, the experimental model was disassembled and carefully examined.

The step by step disassembly of the experimental generator is shown in Figure 1a through 1s. Figure 1a shows the experimental model generator still on its test stand after 2556 hr operation at a T_h of 1200°C in vacuum. Monitoring thermocouples, mounting hardware, voltage and current electrical connections are visible. Upon removal from the test stand, the thorium oxide cored tungsten resistance heater and mounting base (Figure 1b) were found to be in good condition with only slight deterioration of the zircon brick insulating base. The generator itself, pictured in Figures 1c and 1d, had an excellent external appearance and seemed to be structurally sound. The emissive coating (Monsanto Research Corporation's TEC-1) applied in the latter portion of the testing was intact and appeared well bonded.

Actual disassembly was initiated by removing the zircon brick and Fiberfrax insulation (Figures 1e and 1f). All of this material was in good condition and apparently functioning. Although an extensive sintering effect appeared within the insulation itself, no detrimental reaction with adjacent structures was noted. One badly deteriorated molybdenum radiation shield was found (Figure 1g), but all others appeared to be in good condition. Figure 1h shows the stripped generator with removed insulating material in the background.

Removal of the molybdenum foil radiation shield that had been placed between the rows of thermoelements disclosed a major construction problem. These shields originally consisted of four parallel spaced layers of foil. The inner (hottest) layer was found to be almost completely gone with a visible plating deposited on the thermoelectric sections. The second layer was badly warped and partially missing (Figure 1i) with some pieces apparently clinging to the adjoining thermoelectric sections. This bridging

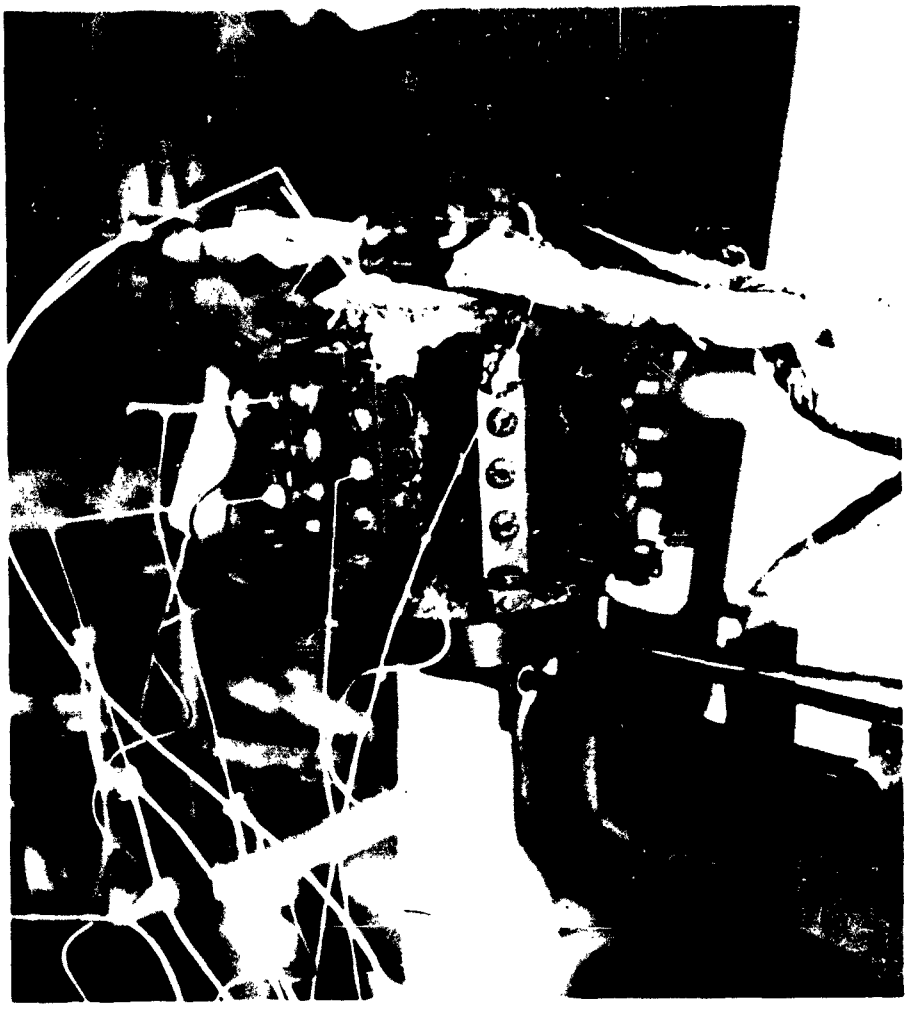

1a Experimental model generator in test stand.

Figure 1. Stepwise disassembly of experimental model generator after 2556 hrs exposure at a T_h of 1200°C in a vacuum.

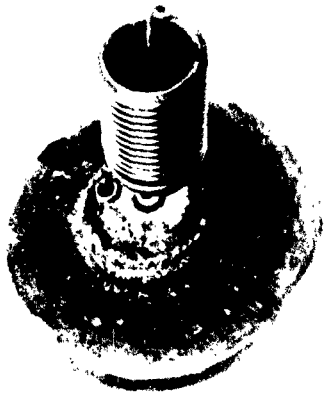

1b Tungsten resistance heater and generator mounting base.

1c Top view of generator, as removed from test stand.

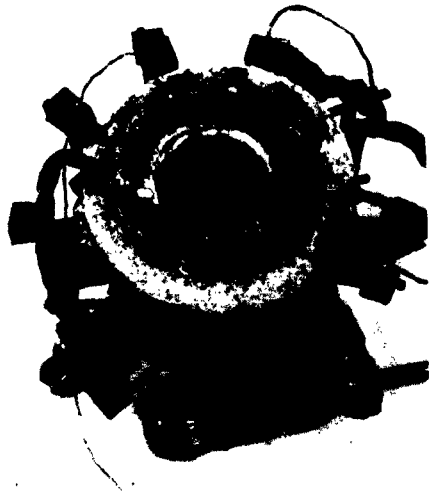

1d Bottom view of generator as removed from test stand.

1e Top view with Fiberfrax and zircon brick insulation partially removed.

1f Bottom view with Fiberfrax and zircon brick insulation partially removed.

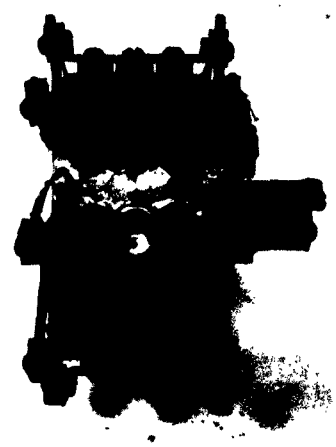

1g Side view showing deteriorated external molybdenum foil shield.

1h Generator with removed insulation in background.

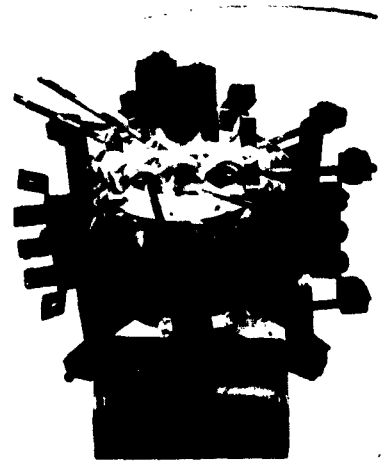

1i Generator with molybdenum shield removed showing deterioration of the inner layers and fragments clinging to sections.

1j Molybdenum shields, as removed, including deteriorated fragments.

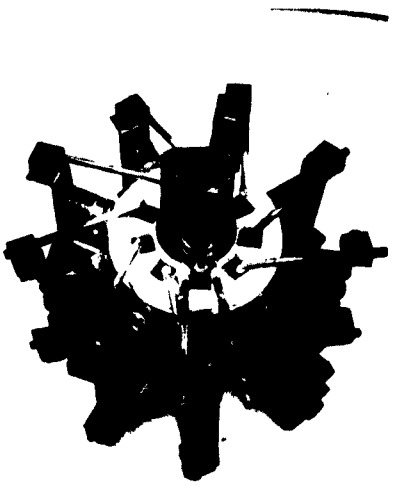

1k Generator with all shields and insulation removed.

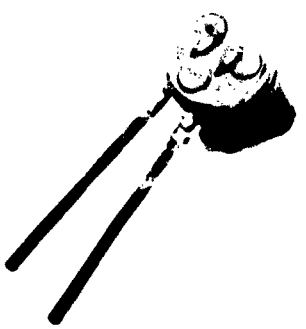

1l Top section as removed, showing extensive plating from the tungsten heater.

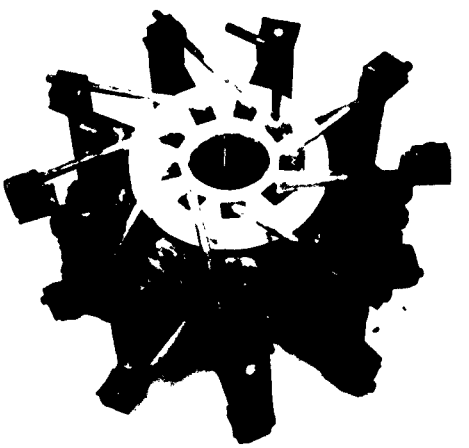

1m Top view of generator with top section removed showing excellent general condition.

1n Detailed view of tungsten heater plating inside generator, taken from the top.

lo Detailed view of tungsten heater plating inside generator, taken from the bottom.

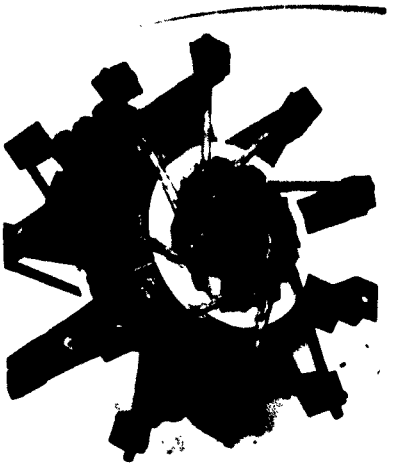

1p Bottom angle view showing good condition of generator between sections.

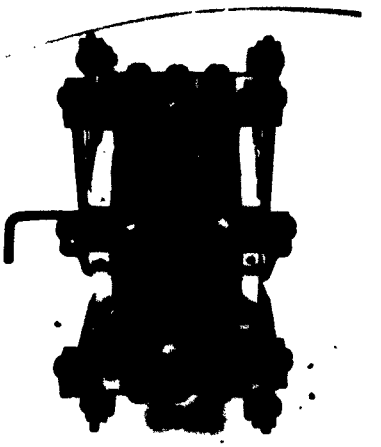

1q Side view showing good condition of generator thermoelements.

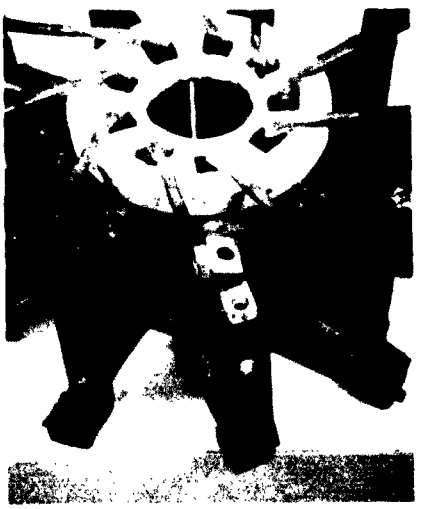

1r Detailed view showing clean copper plate on the molybdenum leads and bright copper electrical connection clamp.

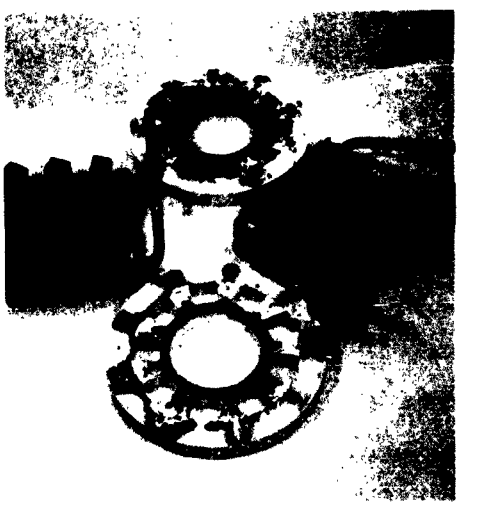

1s Disassembled basic generator structure showing good condition of thermoelectric sections and insulating plates.

of the section would be expected to short them out electrically, resulting in a decreased output. The molybdenum shielding, with collected deteriorated fragments, is shown in Figure 1j as it was removed. The exposed generator structure (Figure 1k) appears to be in very good physical condition and would be expected to regain its original power output if the metal plating were removed and the shielding, insulation, and electrical connections repaired.

The top thermoelectric section of the generator (Figure 1l) appeared to be in good shape when removed, except for the tungsten plating from the heater. The electrical connections were tight and appeared to be making good contact.

The exposed internal surfaces of the model generator were heavily plated with tungsten from the heater with the plating peeling in such a manner as to make definite determination of possible electrical short circuits between sections very difficult. In any case, the plating phenomenon is undesirable. The structural solidarity and metal plating are visible in Figures 1m, 1n, 1o, 1-p, and 1q. Figure 1q affords a view of the particularly good condition of the thermoelements.

Further disassembly of the basic generator disclosed excellent electrical contacts between the molybdenum lead wires and the copper radiator clamps (Figure 1q) with copper metal actually adhering to the molybdenum wire and the bright (clean) copper surfaces welded together. One doubtful connection found at the top clamp of section six was a definite exception. This may have been detrimental to performance, however, since the only structural fault discovered also occurred in section six - a transverse fracture of the graphite connector shoe at the center element. Electrical isolation of one or two thermoelements with their resultant loss to power generation could have occurred here.

All other thermoelectric sections and the electrically insulating boron nitride positioning plates were found to be in good condition (Figure 1s). No physical damage (e.g., cracks, etc.),sublimation, or solid state diffusion damage was discernible.

Most molybdenum lead wires were found to be loose in the graphite section shoes with excessive looseness noted in sections 3, 4, 7, and 8 on the top and section 7 on the bottom. The hypothesis advanced earlier "that repeated insertion and removal of the molybdenum lead wires from graphite section shoes, combined with thermal expansion effect produced when molybdenum-graphite contacts are cooled, results in contacts of increased resistance and lower generator output," is considered to be borne out by this examination. The molybdenum-graphite hot-end contact feature was undoubtedly a major flaw in the experimental model generator design. This problem has been circumvented by the development of n-type thermoelectric materials and sprayed metal electrical connections for the advanced experimental model generator.

In summary, three basic design faults became apparent from this examination of the experimental model generator:

1. Molybdenum lead wires, as fitted into the graphite connector shoes of the thermoelectric sections, are not adequate to resist thermal cycling. This problem has been rectified in the advanced experimental model generator design through the use of new thermoelectric materials and by the formation of electrical connections using flame/plasma metal spraying techniques.

2. Molybdenum radiation shields as exposed to the direct thermal radiation from the heater through the slots between the shoes of the thermoelectric sections in this model were not adequate. The inner shields should have been formed from a more refractory metal such as tungsten for long-time operation in this design. This should not be a problem in the advanced experimental model generator, since our present design does not expose the external shielding directly to the heat source.

3. Vacuum evaporation and plating of metal from the heat source and shields will continue to be a serious problem in the advanced model generator, unless they are circumvented in design. Plating from the shielding has been corrected as outlined in (2) above. Plating of metal from a heat source is not, basically, a generator design problem, but must be considered in the design of test equipment and of the heat source in actual usage. Protection against electrical shorting resulting from metal plating can be provided by coating the inner surface of a generator with a ceramic, such as thorium oxide.

The disassembly and examination of the experimental model generator was helpful in explaining the loss of power output following its disassembly prior to the 2556 hr test, and the avoidance of potential troubles in the design of the advanced experimental model thermoelectric generator.

B. PHASE II - COMPONENT IMPROVEMENT AND EVALUATION

This phase is concerned with the development of standardized MCC 60 (1200°C, n-type) and MCC 40 (900°C, n- and p-type), a new thermoelectric material originated by Monsanto Chemical Company to supplement MCC 50 (1200°C, p-type). Measurements of the thermal efficiency of segmented n- and p-type thermoelements of these four materials are also presented. The results of further efforts to solve junction-forming problems and to develop

fabrication procedures for thermoelements to be used in the advanced experimental model generator are reported, as is the further development of flame and plasma coating techniques of fabricating thermoelements from these new materials. Additonally, the results of emissivity and absorption measurements on a highly emissive radiator coating for use on the radiators of the advanced experimental model generator are presented.

1. Studies of Thermoelectric Materials

The formulations for each of the four thermoelectric materials to be used in fabricating the advanced experimental generator were standardized this quarter. These formulations, selected on the basis of highest power output for ΔT's anticipated for the advanced experimental model generator are presented below:

p-Type Thermoelement	n-Type Thermoelement
MCC 50 with 1 mole % CaO added	MCC 60 with 1 mole % each of CaO, $ThSi_2$ and $ThSi_2$ and Co-Si added
MCC 40 with 0.5 mole % CaO and 0.25 mole % B added	MCC 40 with 0.5 mole % ThO_2 and 2.0 mole % As added

The thermoelectric properties vs. temperature of each of these above thermoelectric materials are presented in Figures 2, 3, 4 and 5. Data for the curves were obtained by measuring the thermoelectric properties of typical hot-pressed bare (without contacts) specimens 1/2" dia. by ~1/2" long. Design of the advanced experimental model generator, as discussed in Section III below was based on data from these curves.

2. Emissive Coating

While effort on this phase was small this quarter, significant results can be reported. Specimens of a phenolic-carbon type coating (coded TEC-1) were subjected to total hemispherical emittance measurements by the Materials Coating Section of the US Naval Radiological Defense Laboratory, San Francisco, with results shown in Figure 6. The curves show that emittances ranging from 0.9 at 500°C to possibly as high as 0.98 at 900°C are attainable with this coating. Such high emittances at elevated temperatures check with the higher ΔT's reported last quarter in tests of this coating on the radiators of the experimental model generator.

The TEC-1 emissive coating is readily applied to copper and other metals and is bonded to substrate surfaces by air-curing followed by a low temperature (200°C) 400°C) thermal bakeout for a few hours in a vacuum.

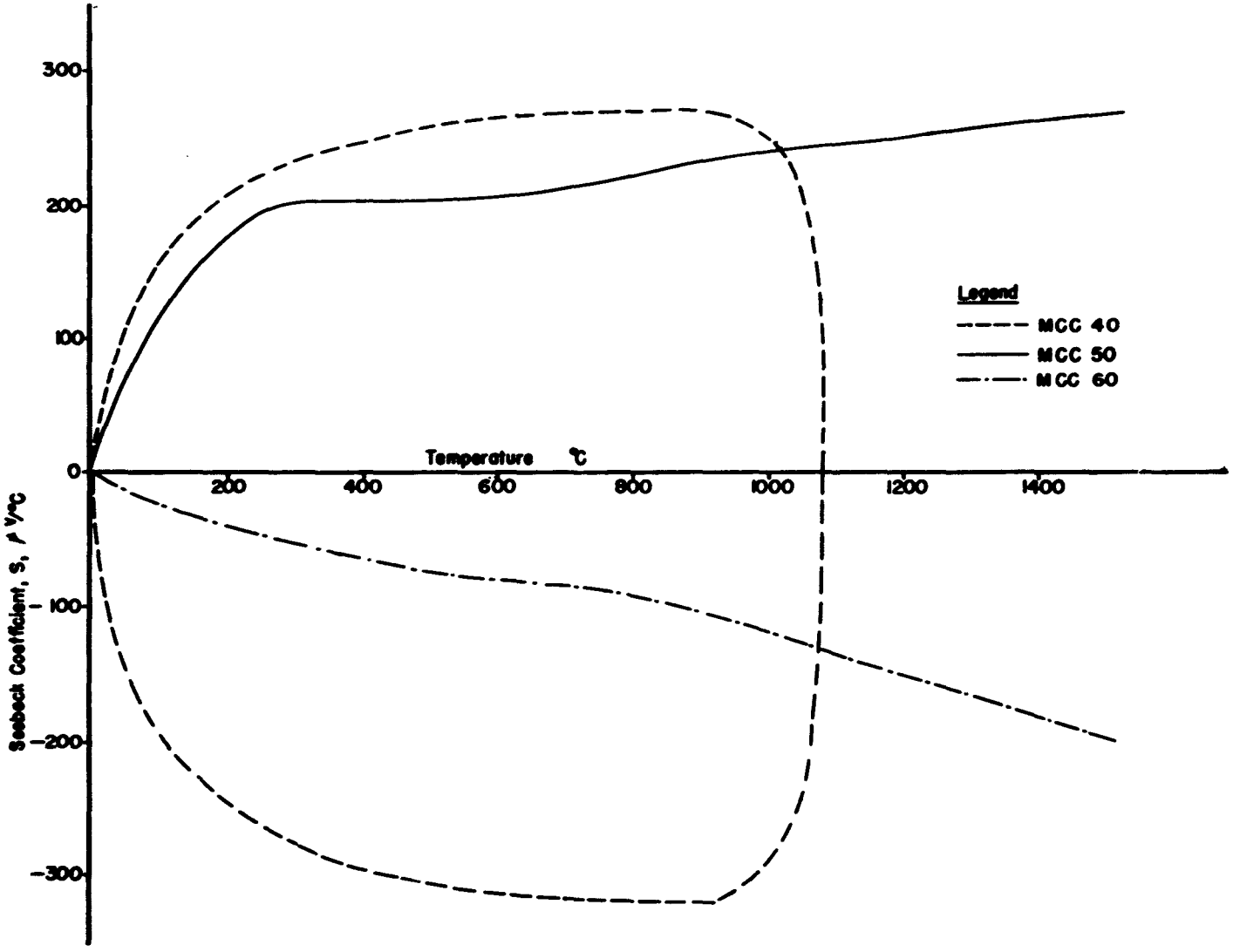

Figure 2. Seebeck coefficients vs. temperature for the thermoelectric materials to be used in the advanced experimental model generator

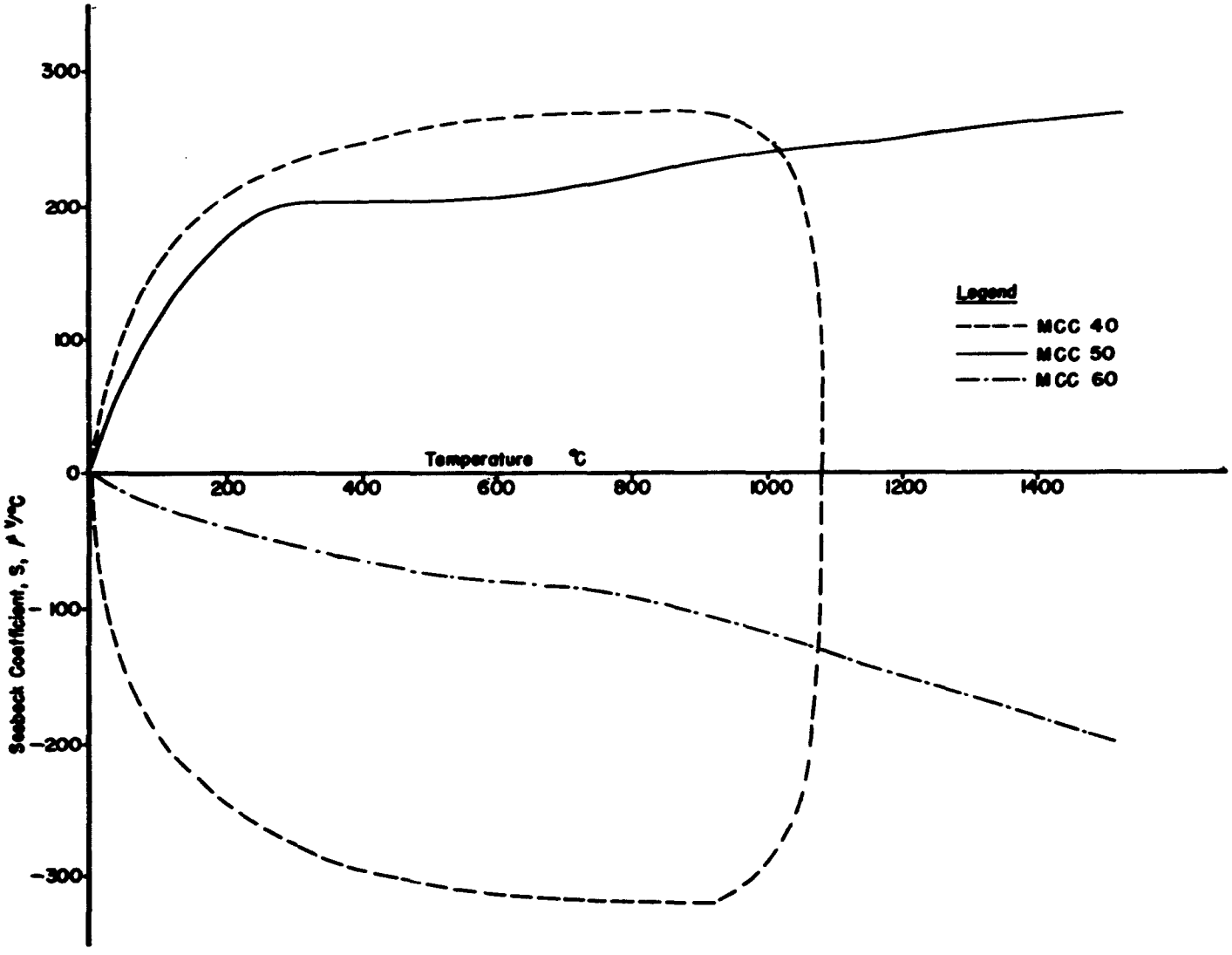

Figure 2. Seebeck coefficients vs. temperature for the thermoelectric materials to be used in the advanced experimental model generator

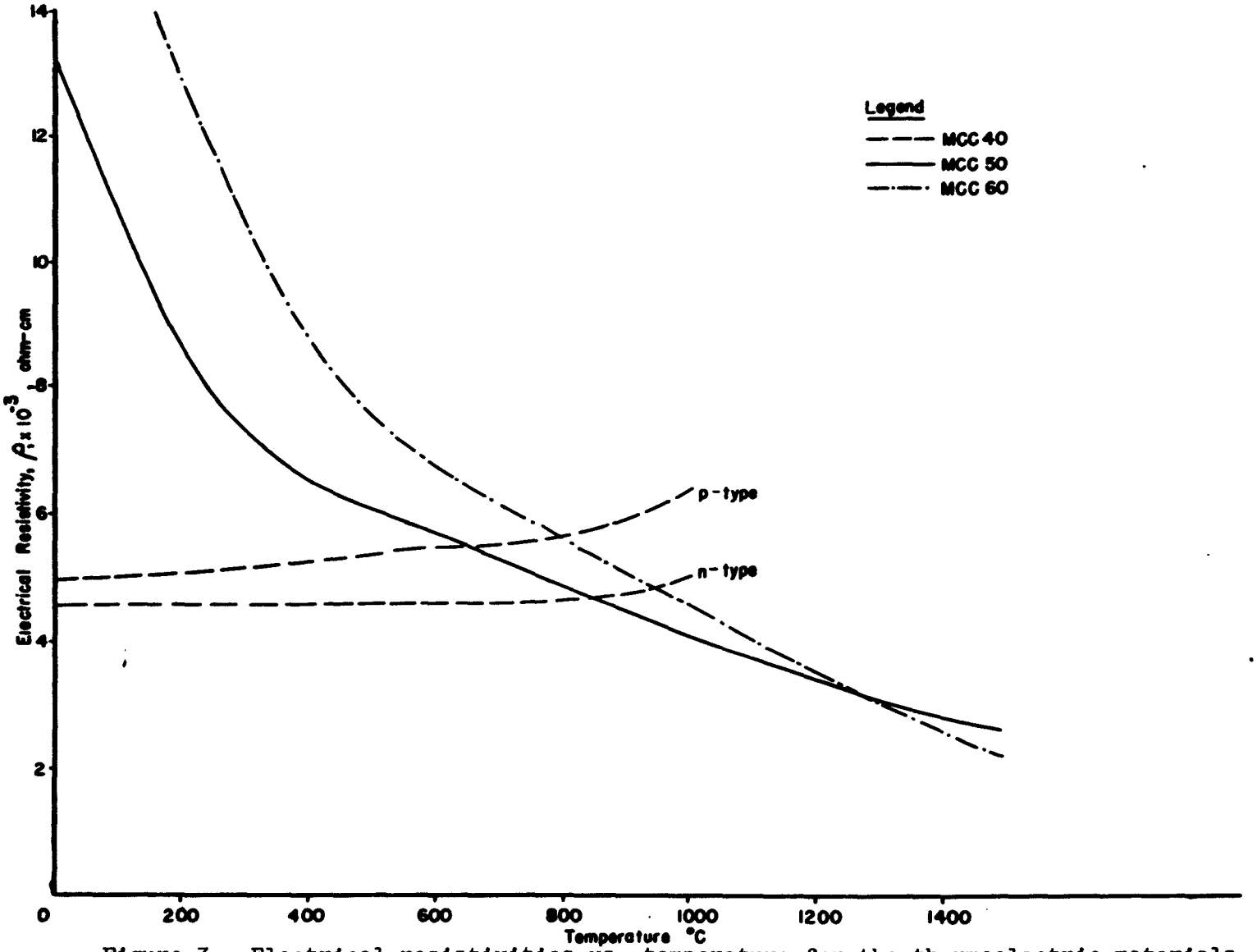

Figure 3. Electrical resistivities vs. temperature for the thermoelectric materials to be used in the advanced experimental model generator.

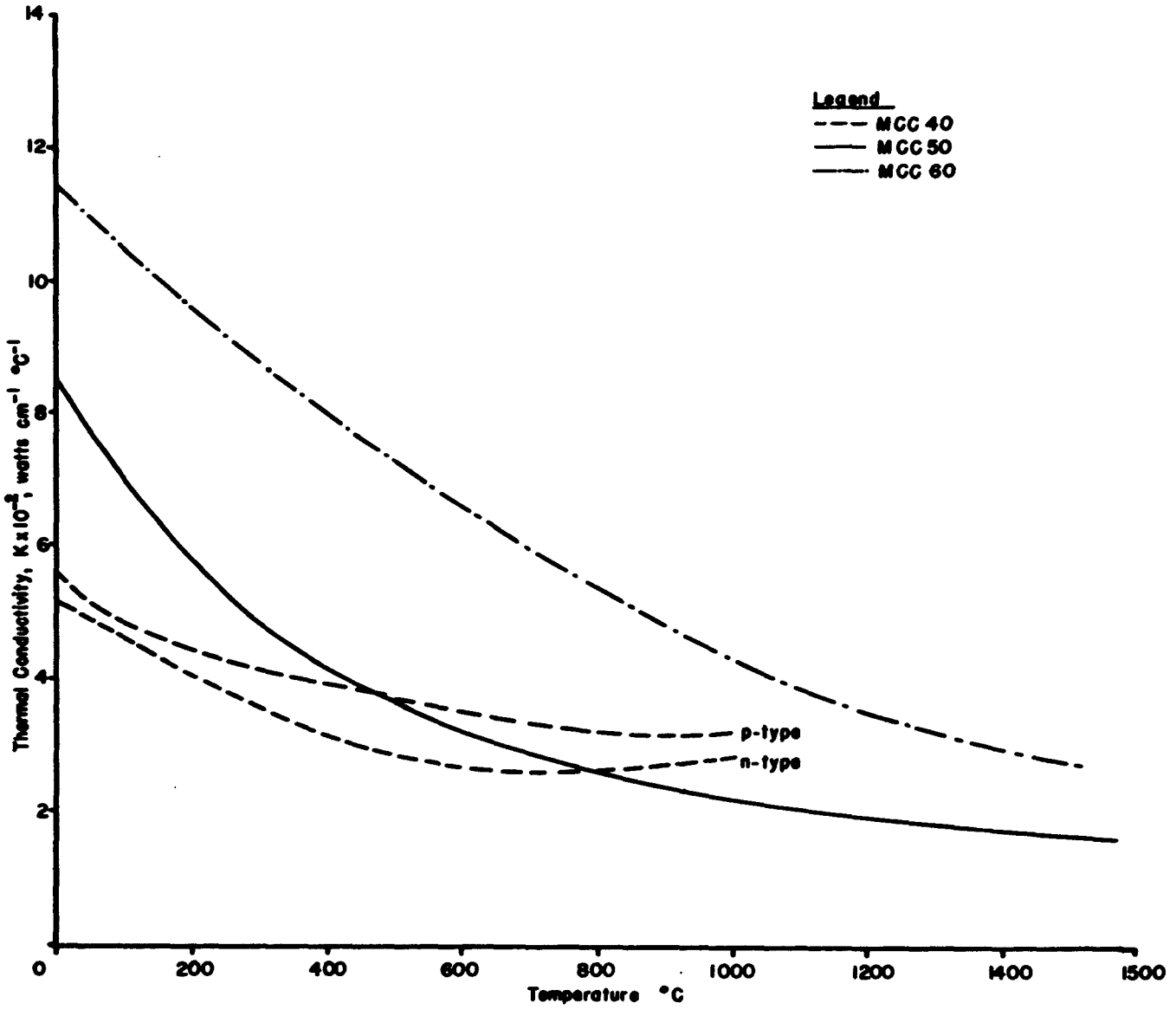

Figure 4. Thermal conductivities vs. temperature of the thermoelectric materials to be used in the advanced experimental model generator.

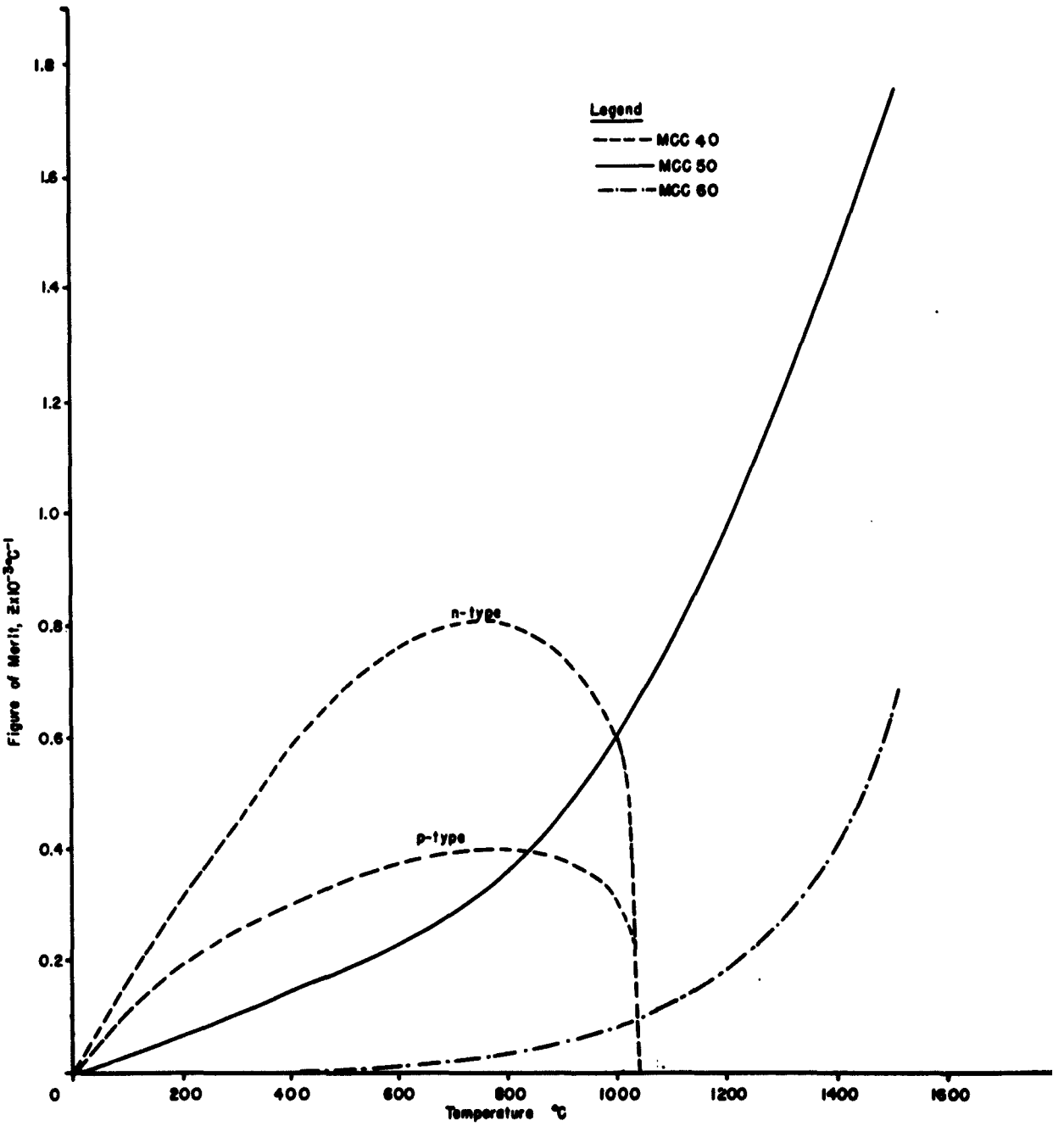

Figure 5. Merit factors vs. temperature for the thermoelectric materials to be used in the advanced experimental model generator.

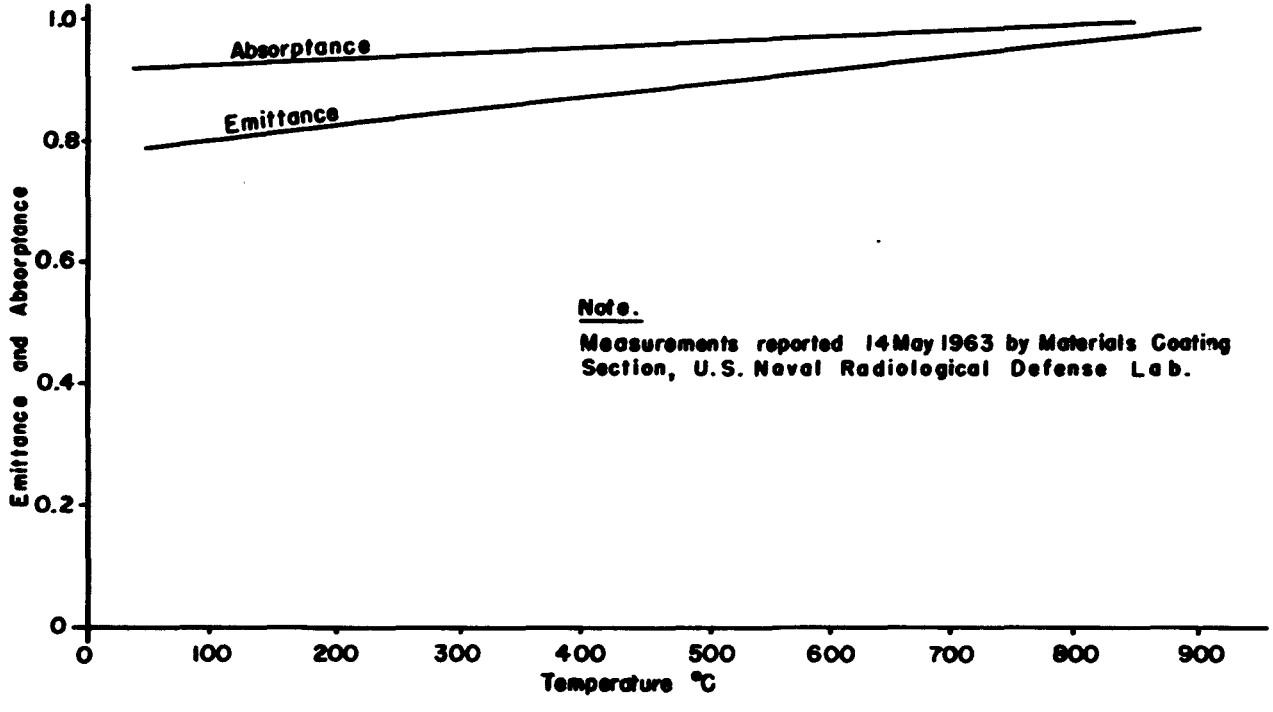

Figure 6. Variation in surface emittance and absorptivity (over a copper substrate) of radiator coating TEC-1 vs. Temperature.

The mechanical bond between TEC-1 and substrates does not appear capable of resisting repeated flexing or severe impact blows, but appears adequate for a good thermal contact with the radiator surfaces of space power units and vehicles. On the basis of findings to date, the TEC coating will be used to provide highly emissive radiators on our advanced experimental model generator.

3. Efficiency Measurements on Segmented Thermoelements

Completion of quantitative emittance measurements on the TEC-1 coating vs. temperature enabled us to devise a technique and apparatus for measuring the actual thermal efficiency of segmented p- and n-type thermoelements of the type to be used in building the advanced experimental generator. This apparatus permitted measurements in vacuum at the anticipated 1200°C-500°C operating temperatures of the generator.

The technique involved attaching a radiator (copper) of known dimensions (5.065 cm^2 area) to the cold end of p- or n-type thermoelements. The surface of the radiator was coated with TEC-1 and fine wire thermocouples were installed in the radiator surface to determine its temperature (Tc, °C). The thermoelement to be tested was mounted vertically, with its hot junction end screwed into a heat source capable of developing 1200°C temperatures. Heat losses from the lateral surface of each thermoelement were minimized by careful thermal shielding. The entire assembly was mounted in a vacuum chamber, with the heat from the coated surface of the radiator rejected to ambient room temperature. Knowing the temperature, area, and emissivity of the radiator, the quantity of heat (Q_2, watts) flowing through each thermoelement could be calculated. Attaching power leads and fine wire thermocouples to the hot and cold ends of the thermoelements permitted the Seebeck coefficient and resistance of the thermoelements, its power output (Q_1, watts) power throughout, and its overall thermal efficiency to be measured.

Data from measurements made on 0.5" dia. segmented p- and n-type thermoelements is presented in Table 1.

The results reported in Table 1 are probably conservative for individual thermoelements. This is believed to be true since it was not practical to completely prevent radiant energy from the heat source from reaching and heating the radiator. The thermal efficiencies of 3.28% and 6% obtained for segmented p- and n-type thermoelements, respectively, appear adequate for reaching generator performance ratios of about 10 watts/lb for anticipated generator operating temperatures.

Table 1. EFFICIENCY OF THERMOELEMENT DATA

Test Item	Thermoelement p-Type	Thermoelement n-Type
Hot-end temperature (T_h), °C	1212.0	1202.0
Cold-end temperature (T_c), °C	473.0	461.0
Temperature differential (T_h-T_c), °C	739.0	741.0
Open circuit voltage (E_{oc}), mv	114.6	201.9
Power out of couple (Q_1), watts	0.264	0.446
Internal resistance, ohms	0.0125	0.181
Seebeck coefficient, μ volts/°C	155	268
Total power through thermoelement (Q_2), watts	8.04	7.41
Overall thermal efficiency, %	3.28	6.01

4. Junction Forming Techniques

a. Hot-Press Fabrication of Thermoelements

Development of fabrication techniques for producing segmented thermoelements to be used in the advanced experimental generator has required major effort this quarter. Initial attempts to make a thermoelement consisting of graphite-MCC 60-MCC 40-graphite met with qualified success. Predicted reactions took place, in most cases, at the MCC 60-MCC 40 interface and resulted in a good mechanical bond. Unfortunately, the electrical resistivity of these reaction products was sufficient to measurably increase the internal resistance of the n-type thermoelement. In the p-type thermoelement, consisting of graphite-MCC 50-MCC 40-graphite, the desired interface reactions occurred rarely and only a few structurally sound elements were produced. These also suffered from a relatively high internal resistance. A considerable number of varying fabrication cycles and metallic and/or ceramic intermediates were attempted in an attempt to produce a reasonable yield of high quality 0.5" dia. elements, on a reproducible basis, by improving the interface reaction and reaction products. No intermediates were produced with better characteristics than those of the graphite-MCC material transitions, so attempts to bond the thermoelectric materials directly were abandoned and a thin (~0.10") graphite intermediate zone was interposed between the materials. This resulted in a system of graphite-MCC 50-graphite-MCC 40-graphite for the p-type element and graphite-MCC 60-graphite-MCC 40-graphite for the n-type thermoelement. Yields of good quality thermoelements were increased to 60-70% in both types, with the remainder rejected because of mechanical failure of bonds or undesirable electrical characteristics. Enough elements were produced by this technique to construct an exploratory 3-tier subassembly containing 12 p-type and 12 n-type

segmented thermoelements of 0.5" dia. Tests on this unit indicated desirability of reducing thermoelement diameter to 0.375" and a corresponding reduction in length, in order to attain a more favorable power-to-weight ratio. When (in cooperation with the project engineer) the decision was reached to use these smaller thermoelements, it was found to be impossible to directly extrapolate the fabrication techniques used for the 0.5" dia. elements (Figure 7).

Numerous nonlinear variables such as temperature distribution in the hot-pressing die, die wall friction, and pressure/consolidation rate ratios reduced initial yields of good quality 0.375" dia. thermoelements to about 10% of attempts. Several weeks of experimentation with these variables was required to regain the 60-70% production yield considered minimal. This 60-70% yield of useful segmented thermoelements is currently obtainable only with 1:1.3 ratios of the lengths of MCC 50:MCC 40 and MCC 60: MCC 40 segments. While this ratio is probably not optimum for maximum power output, it should permit the major design goal of a nominal 10 watts/lb for the advanced experimental model generator to be achieved. We anticipate further improvement in yield as production of units for the advanced experimental model progresses and produces better resolution of process variables through practice-of-the-art.

Fabrication of 24 graphite-junction p- and n-type segmented thermoelements, 0.375" dia., was completed. These units will be used to assemble a new 3-tier subassembly of the advanced experimental model generator. This subassembly unit will be subjected to performance tests while the remainder of the components of the advanced experimental model generator are being fabricated. Information obtained from such tests will be used to provide sustained performance data on the thermoelectric materials selected for the final generator and to discover possible trouble spots in design.

The unexpectedly large number ($\sim$250) of hot-pressings used to solve thermoelement fabrication yield problems consumed a large portion of the boron nitride and graphite die materials acquired for component fabrication in the advanced experimental model generator. Additional materials have been procured, and no delay in completion of the generator is anticipated.

The current technique is described as follows and, graphically, in the flowsheet of Figure 8. The previously prepared formulation for the high-temperature segment of MCC 50 or MCC 60 is loaded into a carefully machined boron nitride liner with AUC electrical-grade graphite male rams. This assembly is positioned in a structural grade (ATJ or Stackpole 331) graphite die which acts as the inductive susceptor. Machining on the bore of the liner and the male rams (which become the thermoelectric junctions) is held to $\pm$ 0.0005". The loaded die is placed in an induction

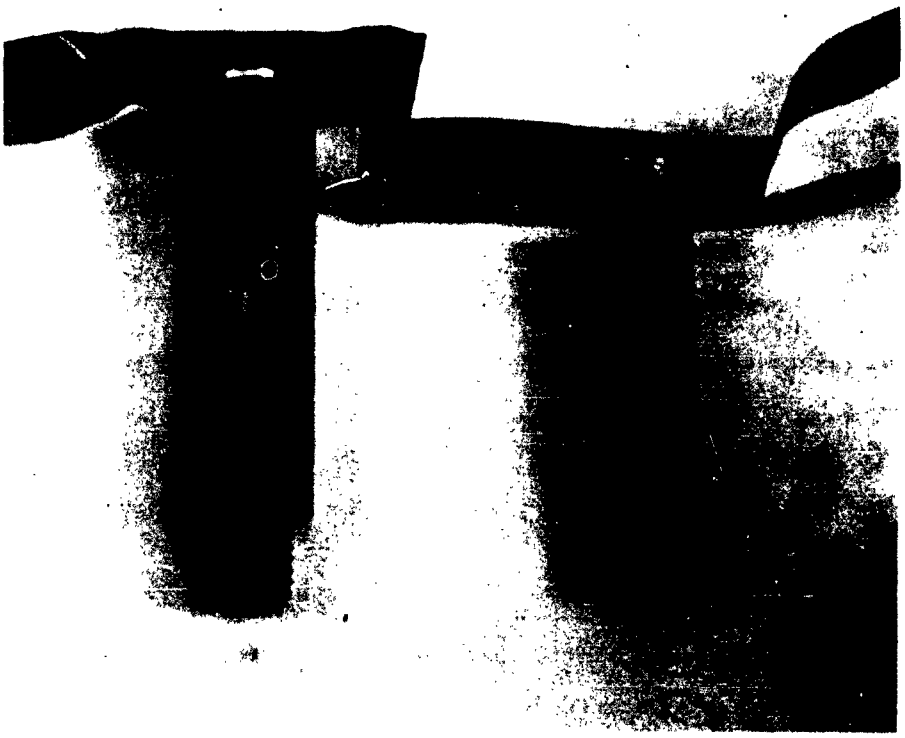

Figure 7. Typical 0.5" diameter and 0.375" diameter thermoelements equipped with temporary radiators for screening purposes.

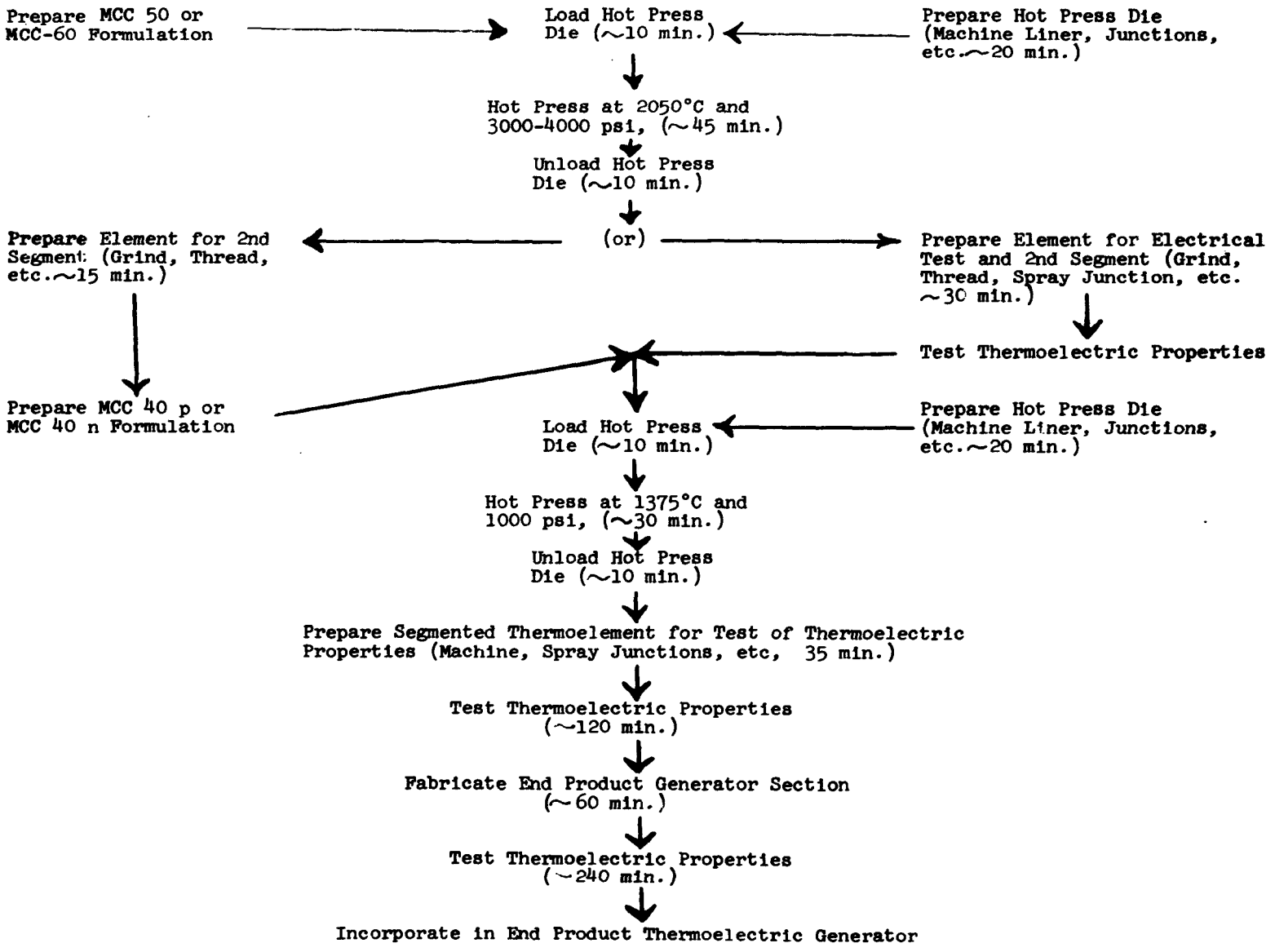

Figure 8. Process flow sheet for fabrication of thermoelements by hot-pressing

furnace and brought to temperature at a rate of 200 °C/minute from ambient. MCC 50 material is subjected to a gradual increase in the ram pressure with temperature, which culminates at 4000 psi at ~ 1900 °C. The maximum temperature of 2050 °C is then attained, as the increase rate continues, and held for 8 minutes. MCC 60 material is subjected to a gradual increase in the ram pressure with temperature, which culminates at 3000 psi at ~1700 °C. The maximum temperature at 2050 °C is then attained, as the increase rate continues, and held for 5 minutes. The thermoelectric formulations react with the graphite male ram during this cycle to form a continuously changing transition zone of reaction products. These products are respectively compatible with each material in both mechanical and electrical characteristics. A strongly reducing carbon monoxide environment in the die, produced by partial oxidation of the die wall, protects the contents while at elevated temperature. The die and element are then cooled to ambient temperature under 1000 psi pressure at a rate of 200 °C/minute.

The high-temperature thermoelement product is removed by cutting away the die and liner. One graphite junction is machined to a 3/8"-24 thread, the outside of the thermoelement is ground to serve as a male ram in a boron nitride liner, and the other graphite junction is removed to ~ 0.10" length from the thermoelectric material and serrated to increase the reactive surface area. This segment is then loaded into a new die and liner as one male ram with a graphite male ram on the other and containing the appropriate and previously prepared MCC 40 formulation. The thermoelectric properties of the high-temperature segment may also be tested as an intermediate step, before loading into the new die, to insure a high quality end product.

The new die, as loaded, is charged into an induction furnace (as before) and the temperature increased at a rate of 200 °C/minute to a maximum of 1375 °C. The maximum temperature is held for 5 minutes. During this period, the pressure is so controlled as to maintain a slow, steady rate of consolidation which will attain a predetermined maximum in the time cycle. Control of this portion of the cycle is extremely critical. After the 5-minute hold at temperature, the die and contents are cooled to ambient at a rate of 200 °C/minute. The pressure is increased with decrease in temperature (as the rate of consolidation permits) until a maximum of 1000 psi is attained at about 1100 °C. The cooling rate is continued to ambient temperature. The thermoelement is again removed, now in segmented form, by cutting away the die and liner.

The resultant thermoelement is then tested for mechanical integrity and thermoelectric properties. If it is found to be of suitable quality, it may be incorporated into a generator subassembly and, eventually, used to fabricate the end product advanced experimental generator.

b. Metallographic Investigation

The difficulty encountered in the hot-pressing junction forming steps suggested a need for a cursory metallographic study to provide more thorough knowledge of the microstructural aspects of this problem. To accomplish this, the thermoelectric components, MCC 40, MCC 50, MCC 60 and their bonds with graphite and with each other,were studied metallographically.

The preparation of these components was quite difficult because of the varying hardnesses of the several phases present in each specimen. All specimens were sectioned with a diamond saw and mounted in Bakelite mounting plastic. Graphite specimens were first smoothed on a belt grinder, then ground on 220, 320, 400, and 600 grit silicon carbide papers and finish polished on a felt lap with levigated alumina. No etchant was used on graphite since the use of polarized light was sufficiently revealing.

MCC 40 was the softest of the three thermoelectric components and consequently more readily prepared. It was smoothed and ground in the same manner as the graphite. Final polishing, however, was done with 30 through 1/2 micron diamond abrasives. Etching was accomplished with the following acid mixture: 10 parts HNO_3; 8 parts HF; and 79 parts $H_4C_2O_2$.

MCC 60 is harder than MCC 40 and more difficult to polish. Its preparation is similar to that of MCC 50 which will be discussed next. Initial smoothing of its surface was done with 230 grit diamond abrasive on a cast iron lap. Intermediate polishing was accomplished with two series of abrasives. In one the sample was polished on cloth laps with 30, 15, and 6 micron diamond abrasives. In the other, 30, 15, 6 and 1 micron diamond abrasives were used on the cast iron lap. Final polishing was accomplished by extensive use of 1 micron and then 1/2 micron diamond abrasive on water lubricated cloth laps. The tendency of these brittle materials to pit made this step very tedious. When a satisfactory surface was finally obtained, both MCC 60 and MCC 40 were etched electrolytically with a 10% HCl solution. A current density of about 1 amp/sq.in. for 10 seconds gave satisfactory results.

Figures 9 and 10 show typical microstructures of MCC 50. The large amount of porosity in Figure 9 may be due in part to the polishing techniques used, but further refinement of this technique will require a large investment in time. More twinning is usually evident than is shown in Figure 10.

Figure 11 and 12 are photomicraphs of MCC 60. A large amount of nonuniform porosity seems to be characteristic of this material. Again a portion of that observed in these figures may be due to insufficient preparation. Both of these photographs, however, were

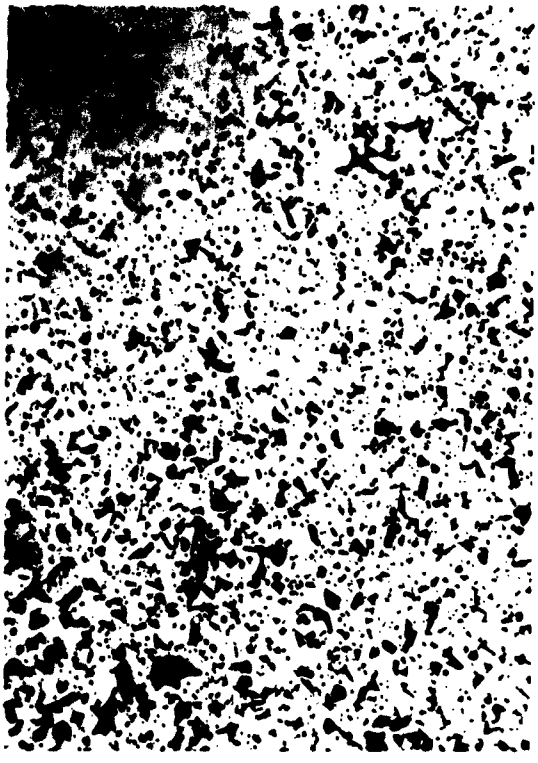

Figure 9. Microstructure of typical MCC 50 specimen, HCl electrolytic etch (100X).

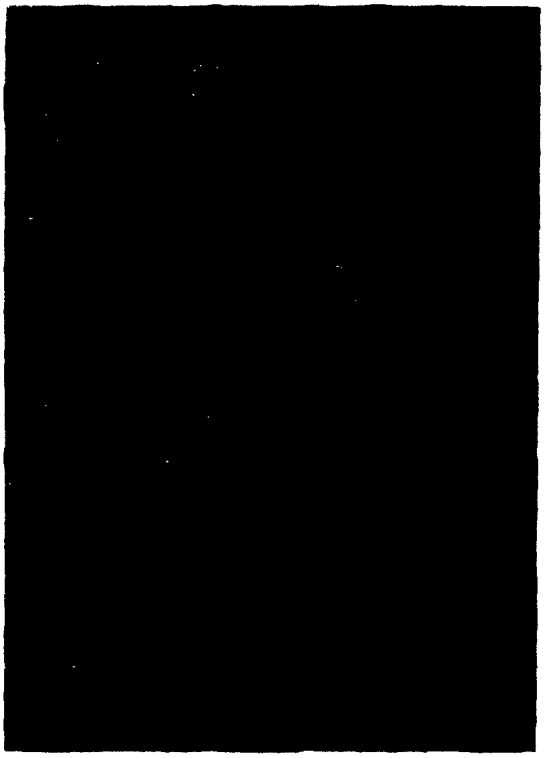

Figure 10. Microstructure of typical MCC 50 specimen, HCl electrolytic etch (600X).

Figure 11. Microstructure of typical MCC 60 specimen, HCl electrolytic etch (100X).

Figure 12. Microstructure of typical MCC 50 specimen, HCl electrolytic etch (600X).

of more dense areas of the specimen. The microstructure of this sample confirms the X-ray diffraction data as to the presence of the cubic modification of the silicon carbide. The reason for the instability of MCC 60 in air was not evident.

The microstructures of p- and n-type MCC 40 are very similar. Figure 13 is a photograph of unetched n-type MCC 40, which shows a fine precipitate of a secondary phase. This precipitate probably results from the large amount of arsenic dopant used in this component, and represents the only major difference in the microstructures of the n- and p-type MCC 40.

Figure 14 is a photograph of unetched p-type MCC 40 and is typical of both the n- and p-type. The very high density of this material is the result of fusion during fabrication; a temperature considerably in excess of the melting point is used. Another characteristic of this structure is a relief polishing effect which appears after final polish on the 1/2 micron diamond abrasive. The lighter appearing areas are softer. Figure 15 is a photomicrograph of etched p-type MCC 40. A great variation in grain size is apparent. The smaller grains tend to favor the softer areas, apparent by relief polishing and the precipitate of the n-type MCC 40 specimens.

The next phase of the investigation dealt with the bonds between the various thermoelectric components and the graphite end plugs. Figure 16 is a photograph of an MCC 60-graphite bond. The extreme porosity of the MCC 60 is the only outstanding characteristic. In Figure 17, a similar picture of an MCC 40-graphite bond, penetration of MCC 40 into the graphite is very evident. In some cases the penetration extended through the entire end plug. In most cases an extruded layer of MCC 40 was also formed on the outside surface of the end plug. Figures 18 and 19 are photomicrographs of MCC 50-graphite bonds. The MCC 50 is the only one of the three thermoelectric elements of this investigation which is affected by the graphite. The effect is characterized by a more dense nonetching material next to the graphite boundary. The cause of this effect and whether it affects the thermoelectric properties of MCC 50 are unknown.

Little difficulty was experienced in bonding MCC 40 and MCC 60 for n-type couples. Figure 20 is a picture of this bond (the MCC 40 is on top). The unetched structure is shown since no variation due to the bonding was observed on etching. The massive white material in the MCC 60 segment appears to be MCC 40. The fact that this material in concentrated in the portion of the MCC 60 segment nearest the bond, that its microhardness is the same as that of MCC 40, and that it etches in a similar manner to MCC 40, support this conclusion.

Many attempts were made to bond p-type MCC 40 to MCC 50. Figure 21 shows photomicrographs of some of these bond attempts. (In all cases the MCC 40 segment is on top). The first picture, 21a,

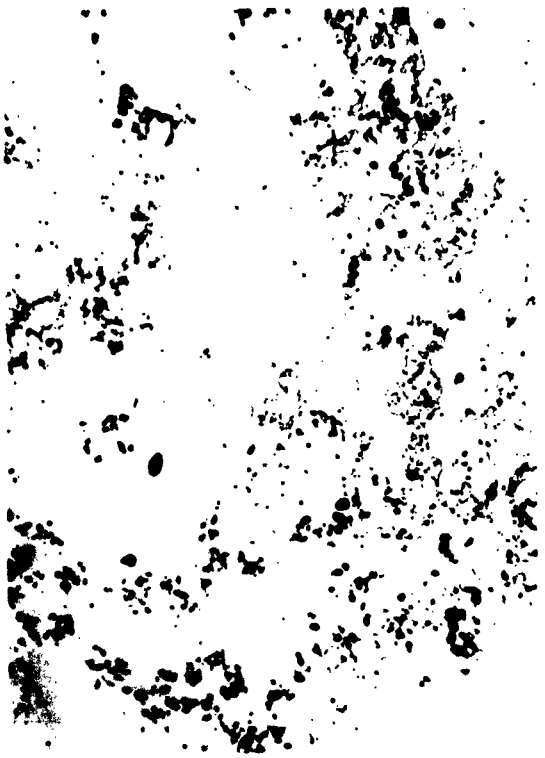

Figure 13. Microstructure of typical MCC 40 (n-type) specimen, as polished (100X).

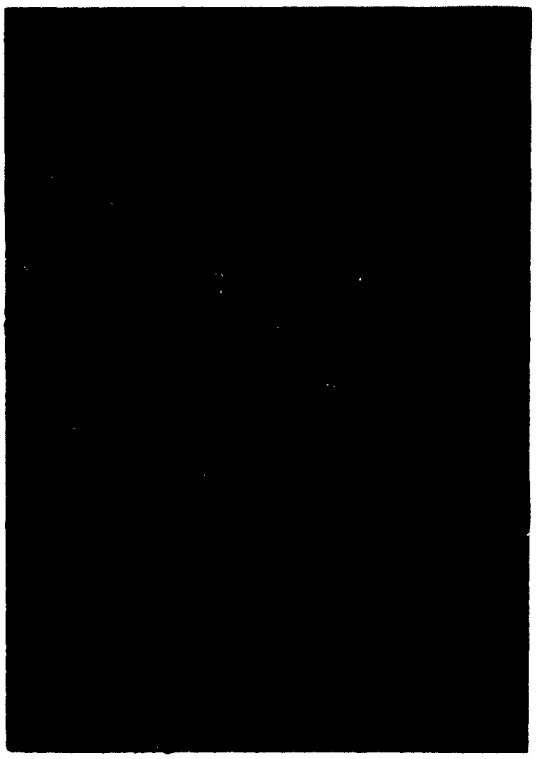

Figure 14. Microstructure of typical MCC 40 (p-type) specimen, as polished (100X).

Figure 15. Microstructure of some MCC 40 specimens (p-type) shown in Figure 14, mixed acids etch (152X).

Figure 16. Microstructure at interface between MCC 60 (light-colored material) and graphite (100X).

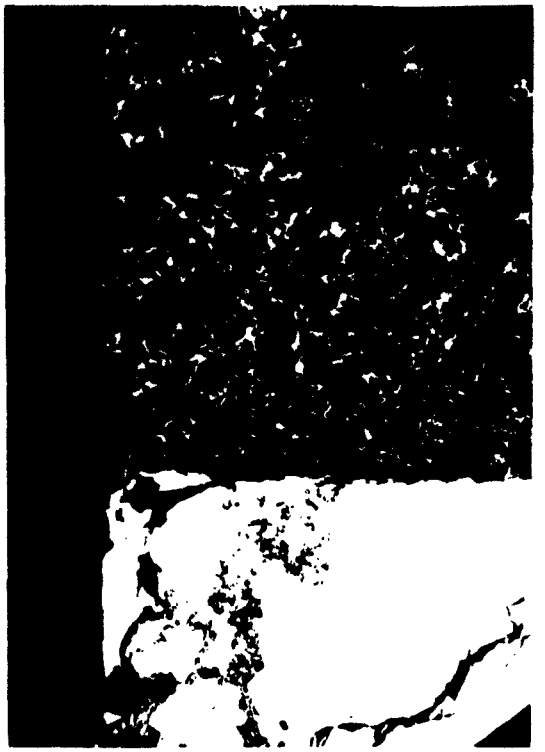

Figure 17. Microstructure at interface between MCC 40 (light-colored material) and graphite, as polished (50X).

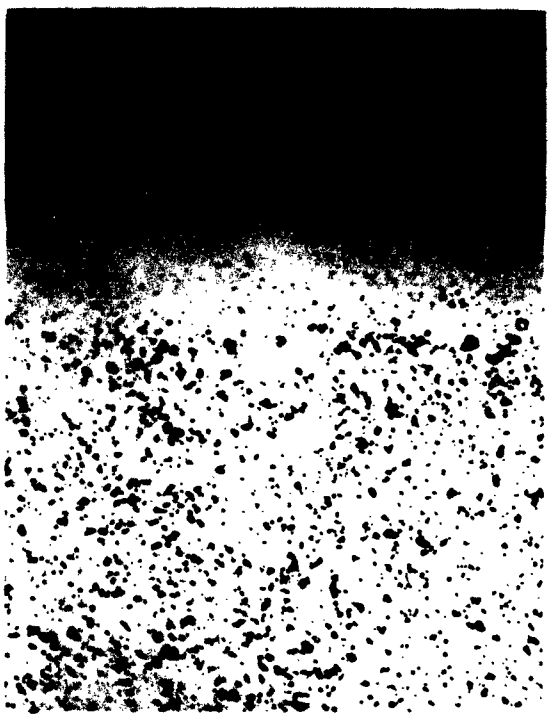

Figure 18. Microstructure at interface between MCC 50 light-colored material) and graphite, as polished (100X).

Figure 19. Microstructure at interface between MCC 50 (light-colored material) and graphite, HCl electrolytic etch (128X).

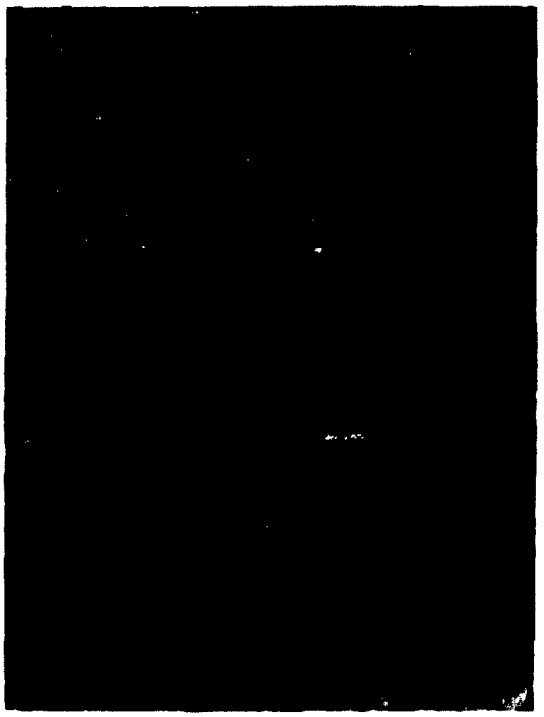

Figure 20. Microstructure at interface between MCC 40 (light-colored material) and MCC 60 in an n-type couple, as polished (100X).

(a) Specimen SM-1 (100X)

(b) Specimen SM-22 (152X)

(c) Specimen SM-61, (256X)

(d) Specimen SM-56 (100X)

Figure 21. Microstructure at interface betw
MCC 40 (p-type) and MCC 50 of
several p-type thermoelements.

specimen SM-1 was a bond made using powdered iron as the intermediate. Upon etching, this specimen revealed a decrease in MCC 50 grain size near the bond indicating some interaction. The next picture, 21b of specimen SM-22, was of a normal procedure bond with no intermediate. The small white particles in the MCC 50 appear to be MCC 40.

The next specimen, SM-61, shown in Figure 21c, was made using platinum foil as the intermediate. The center portion of this picture is platinum or a platinum-rich phase and appears to be bonded well to both the MCC 40 and MCC 50. The angular white precipitate in the MCC 50 is probably a platinum boride. Figure 21d shows a bond made at 1700°C. The transition are in the photomicrograph is typical of high temperature bonds between these materials. None of the above bonds were consistent enough for this application. Since graphite was successfully bonded to both MCC 40 and MCC 50, its use as an intermediate seems logical. An MCC 50 module was made in the normal fashion. Then most of one graphite end was removed and the remaining portion cross-hatched with a hacksaw. Next this cross-hatched end was bonded to the MCC 40 segment by normal hot pressing. Figures 22 and 23 are photographs of the bond area between MCC 50 and MCC 40 produced in this fashion. Notice the continuity of the graphite intermediate between the two thermoelectric materials. The graphite is shown as the light-colored sawtooth-shaped material in the center of Figure 22 and it is seen as horizontal bond extending across the middle of Figure 23.

c. Flame and Plasma Studies

As discussed in the proposal for this project and in earlier quarterly reports, the sizable heat losses and fabrication costs characteristic of designs based on radially mounted hot-pressed thermoelements could be significantly reduced if continuous doughnut-shaped thermoelements of the high temperature thermoelectric materials could be produced by flame or arc-plasma spray methods to yield units like that shown in Figure 24. Successful flame or plasma fabrication techniques would also provide greater flexibility in the shape and capacity of thermoelectric generators. By closely spacing the saw cuts between the segmented adjacent p- and n-type thermoelements of Figure 24, large or optimized L/A ratios for each thermoelement are attainable, and many stages (for higher voltage output) can be produced. Thermoelements extending 360° or completely surrounding the central heat source cavity offer high current capabilities and redundancy of generator circuits. Such combinations of high current and voltage capabilities, coupled with better thermal efficiency obtained through reduced heat losses (as compared with radially mounted hot-pressed cylindrical thermoelements), could provide generators of very high power/weight ratios.

Figure 22. Microstructure at interface between MCC 50 and MCC 40 (p-type) joined with graphite (light-colored saw-toothed material), specimen SM-71 (6.5X).

Figure 23. Enlarged (50X) view of microstructure of specimen SM-71, shown in Figure 22.

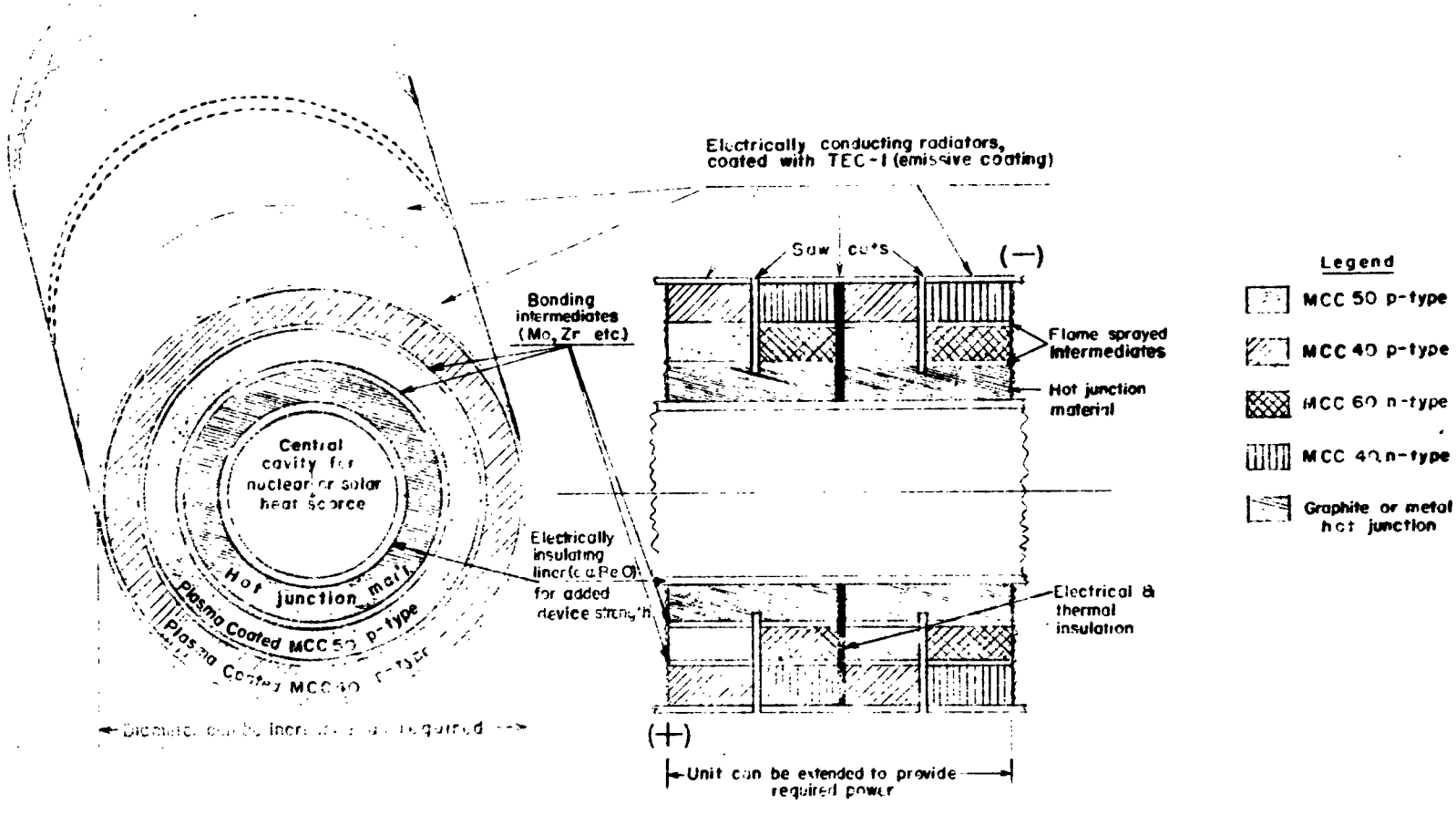

Figure 24. Early conceptual design of flame and arc-plasma fabricated thermoelectric device.

Development of plasma-spray techniques to produce segmented thermoelement assemblies like those shown in Figure 24 is the ultimate objective of this phase of the project. Additionally, and of more immediate importance to the fabrication of the advanced experimental model generator, plasma techniques were developed for improving thermal and electrical contacts at the hot and cold ends of the segmented thermoelements made by hot-pressing methods.

Effort this quarter was directed toward spray-coating MCC 60 and MCC 40 materials, in addition to MCC 50. Previous efforts were primarily concerned with spray-coating MCC 50.

Using powder produced from hot-pressed p-type MCC 40, a sandwich-type thermoelement was produced by plasma spray techniques. This unit, shown in Figure 25, consisted of p-type MCC 40 sprayed upon a substrate of graphite as its hot end contact. Copper was then flame-sprayed upon the MCC 40 to produce a radiator. Electrical leads were attached to the cold side of the unit. Leads must be attached to the hot side before electrical tests on this unit can be conducted.

A thermoelement produced by plasma spraying a mechanical mixture of p-type MCC 40 modified with 0.05 mole % calcium oxide and 0.250% boron is now ready for attachment of leads prior to determining thermoelectric properties.

Efforts were made to produce MCC 60 deposits on graphite using the arc-plasma technique. Using fine powder (about 8μ), a dense coating was obtained which appeared to be satisfactorily bonded to the graphite cylinder.

As shown in Figure 26, a thick (3/16" - 7/32") layer of MCC 50 was plasma-sprayed on a cylindrical 7/16" x 1-5/16" long graphite cylinder. The heavy deposits at each end of the specimen resulted from excess deposits of sprayed material caused when the traversing mechanism used to move the plasma gun hesitated during reversal of its direction during the spraying operation. The threaded graphite portion shown on this specimen was used to mount the unit in apparatus for rotating the cylinder during spraying. The threaded section can also be used as a hot-end connection during evaluation of the thermoelectric properties of the specimen.

The radial cracks seen on the end of the specimen are believed to have resulted from severe thermal shock experienced when the specimen was suddenly subjected to the full energy of the plasma unit when the traversing mechanism was accidentally stopped during the coating operation. Such radial cracks would not be particularly harmful to the performance of a generator fabricated by this technique since power is produced by energy flowing radially from the centrally located heat source. Poor bonds between the hot and cold junctions and the segments, or concentrically position cracks in the segments, would be quite objectionable.

Figure 25. Prototype sandwich thermoelement fabricated by plasma coating techniques.

Figure 25. Prototype sandwich thermoelement fabricated by plasma coating techniques.

Figure 26. Heavy (3/16"-7/32") coating of MCC 50 applied to a 7/16" diameter graphite cylinder by arc-plasma methods.

The properties of molybdenum coatings as produced by arc plasma and flame spraying were briefly studied to select most suitable techniques for producing sprayed hot junctions on p- and n-type couples for use in the advanced experimental model generator. As shown in Table 2, arc plasma coatings were more dense than flame-sprayed coatings, however excessive substrate overheating was encountered. Joints produced with metallizing equipment possessed satisfactory thermal stability and sufficiently low electrical resistance for this application and additionally minimized the possibility of damaging the lower melting components of segmented thermoelements during junction forming. Consequently, this method has been utilized for fabricating hot junctions in p-n samples for evaluation.

Table 2. PROPERTIES OF ARC-PLASMA AND FLAME SPRAYED MOLYBDENUM

		Molybdenum		Coating Properties (after grindin		
Sple	Spray Gun	Type	Size	Thick-ness (mil)	Density	Theo. Density (%)
111	Arc-Plasma**	Powder	-150+325 mesh	7.5	9.10	89.2
112	Arc-Plasma**	Powder	-150+325 mesh	20.0	8.96	87.8
115	Metallizing***	Wire	.125" dia.	16.5	8.29	81.3
118	Metallizing***	Wire	.057" dia.	15.5	8.45	82.9
120	Thermospray***	Powder	-150+325 mesh	4.0	5.10	50.0

* required for accurate measurment of these properties
** 5% hydrogen-argon
*** oxygen-acetylene

Figure 27 shows a prototype thermoelement consisting of concentric plasma sprayed layers of molybdenum, MCC 50, MCC 40 (p-type) and copper on a 7/16" dia. x 1" long graphite cylinder. The layers of spray coated materials on this specimen are somewhat thin to develop the Δ T's needed for optimum efficiency. Even these thin layers could be made to produce useful power by sawing them into thin discs to provide thermoelements with high L/A ratios. However, thicker concentric layers would be more desirable for improving the thermal efficiency of generators based on the flame spray fabrication approach.

Figure 27. Prototype segmented thermoelement produced by plasma coating concentric layers of molybdenum, MCC 50, MCC 40 (p-type), and copper on an inner graphite cylinder.

Alumina and beryllia coatings were also applied to graphite substrates by arc-plasma spraying methods. These specimens were subjected to 1200°C temperatures in a vacuum of 10^{-5} mm Hg for more than 100 hr. This work was done to determine whether alumina and beryllia could be used as electrical insulation in contact with graphite on the hot-end sections of the advanced experimental model generator when it is operating at 1200°C in a vacuum. These studies indicated that neither material reacts with graphite and both exhibited good mechanical strength and resistance to thermal shock.

It is now possible to apply each of the p- and n-type thermoelectric materials studied on this contract to substrates of graphite and spray-coat to produce thin segmented-type thermoelements by plasma coating techniques. However, much further development effort on plasma coating techniques are needed to:

(1) increase the thickness of the layers of the thermoelectric materials

(2) measure the thermoelectric and power-producing characteristics of typical thermoelements

(3) to improve the thermoelectric properties of spray-coated thermoelements to match or exceed those for hot-pressed units

(4) develop cutting, insulating and other techniques that will be used in fabricating generators from plasma-sprayed thermoelements

Additionally, a smaller plasma gun unit and an enclosed (nitrogen or argon purged) spray chamber is needed to minimize oxidation problems now experienced in spraying some junction and thermoelectric materials.

5. Sustained Testing

Sustained performance tests, initiated last quarter on the first p-n couple constructed of 0.5" dia. segmented thermoelements, were extended to 256 hr this quarter. A 4-thermoelement module was constructed and tested continuously for 282 hr. Additionally, sublimation loss determination runs were completed on MCC 60 and MCC 40 materials, and 1200°C compatibility tests were made between beryllia and columbium-zirconium alloy. Details of this work are reported below.

Figure 28 shows the p-n couple test configuration used for the 256 hr sustained test (See Table 3 for data) of the couple constructed of 0.5" dia. segmented p- and n-type thermoelements. The flat circular plate surrounding the two vertical thermoelements at their

Figure 28. Test apparatus used to evaluate the performance of segmented thermoelements as a 2-element module.

Table 3. DATA FOR SUSTAINED TEST ON A TWO-THERMOELEMENT (0.5" DIA.) SEGMENTED p-n COUPLE

Hours of Operation	Average Hot End Temperature, °C	Average Cold End Temperature, °C	Average ΔT Across Couple, °C	Couple Characteristics Under Approximately Matched Load				Open Circuit Potential, mv	Seebeck Coefficient, μv/°C	Vacuum, mm Hg x 10^{-5}
				Current, amp	Potential, mv	Power, watts	Internal Resistance, ohms			
1	1176	417	759	4.56	162.5	.741	.0359	326.4	430.0	.56
16	1178	409	769	4.87	167.6	.816	.0357	341.5	444.1	.40
36	1173	408	765	4.93	170.7	.842	.0353	344.7	450.6	.20
58	1171	408	763	5.00	170.5	.852	.0354	347.6	455.5	.20
64	1173	408	765	5.01	170.5	.854	.0354	348.0	454.9	.20
90	1174	409	765	5.00	172.8	.863	.0354	349.8	457.3	.20
92	1192	412	780	5.09	178.4	.908	.0349	356.2	456.7	.38
110	1201	415	786	5.12	180.6	.925	.0348	358.6	456.2	.45
117	1200	414	786	5.10	180.9	.923	.0347	358.0	455.5	.30
134	1214	417	797	5.21	184.2	.960	.0346	364.3	457.1	.30
141	1200	417	783	5.13	184.9	.948	.0341	359.8	459.5	.30
159	1200	416	784	5.12	183.2	.938	.0354	364.7	459.3	.30
184	1199	414	785	5.13	182.6	.937	.0334	354.0	451.0	.28
208	1198	415	783	5.11	184.1	.940	.0337	356.1	454.8	.30
231	1195	416	779	5.15	183.4	.944	.0349	363.2	466.3	.30
256	1184	414	770	5.07	180.2	.914	.0356	360.5	468.2	.30

approximate midpoints is the top of the high temperature source used to maintain the hot ends of the couple at 1200°C. The two thermoelements were connected by a graphite hot strap (not shown) below the circular top plate. Temperatures of the cold ends of each thermoelement were measured by thermocouples inserted into holes drilled through the rectangular-headed copper screws used to hold the thin (0.010" thick) copper radiators in place on top of each thermoelement. The hot junction temperature of each thermoelement was measured by a thermocouple inserted in holes drilled in the graphite within 0.03" of the interface between the graphite and the thermoelectric materials on the hot ends of each thermoelement. The top surface of each 0.5" wide by 1" long radiator was covered with emissive coating TEC-1.

The p-type thermoelement (the lighter-colored one) consisted of an 0.5" dia. x 1.2 cm long segment of calcium oxide (1 mole%) modified MCC 50. This segment was bonded to graphite at its hot end. An MCC 40 (p-type) segment 0.5" dia. by 1.2 cm long was bonded to the MCC 50 segment and joined with graphite at its other end. The MCC 40 segment was modified with 0.5 mole % calcium oxide and 0.25 mole % boron.

The n-type thermoelement consisted of a 0.5" dia. by 1.2 cm long segment of MCC 60 with 1 mole % each of calcium oxide and thorium disilicides bonded to graphite on the hot end and to an 0.5" dia. x 1.2 cm long MCC 40 (n-type) segment on its other end. The MCC 40 segment was joined to graphite at its cold end.

From the data in Table 4 it is apparent that the performance of the segmented thermoelements remained relatively constant throughout the 256 hr test. Additionally, the importance of operating to the highest feasible (with regard to sublimation losses) hot-end temperatures and ΔT's per thermoelement is also shown. For example, increasing the average hot end temperature and ΔT from 1176°C and 1159°C, respectively, to 1214°C and 797°C, respectively, improved the power output of the couple by almost 30% (from 0.741 to 0.960 watt).

While such improvement in power output with higher operating temperature largely reflects the effect of higher temperatures on the merit factors of thermoelectric materials, it should be noted that more heat was pumped through each thermoelement than is indicated by the cold end temperature of the couple at the 1-hr and the 134-hr time periods. This occurred because a large portion of the total heat flowing through each thermoelement was rejected by the exposed (area projecting above the circular plate) surfaces on the cold end of each thermoelement. No attempt was made to calculate the relative portions of heat rejected from the cylindrical sides of each thermoelement and its radiator, since the surface emissivities of the MCC 40 material are unknown at present.

Table 4. TEST DATA ON A FOUR-THERMOELEMENT (0.5" DIA.) SEGMENTED p-n MODULE

Hours of Operation	Average Hot End Temperature, °C	Average Cold End Temperature, °C	Average / T Across Couple, °C	Couple Characteristics Under Approximately Matched Load				Open Circuit Potential, mv	Seebeck Coefficient, μv/°C	Vacuum, mm Hg x 10^{-5}
				Current, amp	Potential, mv	Power, watts	Internal Resistance, ohms			
1	1200	459	741	9.67	161.3	1.560	.0169	325.5	439.3	.9
17	1203	459	744	9.67	160.0	1.550	.0171	325.5	437.3	.4
41	1202	461	741	9.66	160.9	1.550	.0171	326.5	440.7	.30
68	1210	461	749	9.59	169.1	1.620	.0167	329.4	439.8	.30
94	1193	559	734	9.44	167.5	1.580	.0168	325.8	443.9	.38
113	1196	458	738	9.50	166.6	1.580	.0168	326.4	442.3	.33
137	1206	461	745	9.54	167.2	1.600	.0171	330.7	443.8	.33
160	1206	461	745	9.59	167.9	1.610	.0171	332.4	446.1	.38
185	1207	462	745	9.50	169.1	1.610	.0173	333.5	447.6	.32
211	1207	463	744	9.57	169.3	1.620	.0172	333.8	448.6	.36
235	1205	464	741	9.58	170.0	1.630	.0171	334.6	451.6	.40
266	1207	464	743	9.60	171.9	1.650	.0171	335.5	451.5	.30
282	1208	464	744	9.68	171.1	1.660	.0171	336.6	452.0	.30

Sustained tests to 282 hr were also run on the 4-element p-n module shown in Figure 29. The p- and n-type thermoelements of this module are fabricated from the same formulations used to produce the 2-thermeoelement couple for which test data is reported in Table 3.

Electrically, this 4-thermoelement module consisted of two p-type and two n-type thermoelements connected in parallel, with each pair of parallel-connected thermoelements connected in series by means of a graphite hot plate (not shown) located beneath the circular top of the 1200°C heat source, shown as the large cylindrical object at the bottom center of this figure. As with the 2-thermoelement couple, no attempt was made to reduce the weight of the electrical connections at either the hot or cold ends of the 4-thermoelement module. Thermocouples were installed as close as possible (about 0.03") to the interface between the graphite and thermoelectric materials at the hot and cold ends of the thermoelements. The top surface of the 0.5" wide by 1.5" long thin (0.01") copper radiator mounted across the top of each pair of thermoelements was coated with TEC-1. As in the 2-thermoelement couple test, the MCC 40 segments and graphite at the cold ends of the thermoelements were exposed to ambient room environment. Table 4 presents the data obtained in the sustained tests on this 4-thermoelement module.

Here, as with the 2-thermoelement couple, the power output of this module remained relatively steady with time, and making allowances for the lower ΔT's across the thermoelements (compared with ΔT's on the 2-element couple) the power output per thermoelement approached that obtained in the tests on the 2-element couple.

Longer performance tests (1000 hr) will be run next quarter on a 2-thermoelement couple constructed from the standardized materials characterized in Figures 2, 3, 4 and 5.

Sublimation tests were continued this quarter on MCC 60 and MCC 40 thermoelectric specimens. The test data on a typical MCC 60 specimen 16-1-N is presented in Table 5.

Based on the test data in Table 5 and the lower average operating temperature of the segment in a generator, it is estimated that the sublimation losses of the MCC 60 segments of the thermoelements for the advanced experimental model generator will be less than 3% in a 12-month period. When used in a generator, the MCC 60 segment will operate between 1200°C and 850°C, or at significantly lower average temperatures than used in the above test. On the assumption that the bulk of the total loss occurs at the 1200°C interface between the MCC 60 and the graphite hot lead and a decreasing sublimation rate with time, it is estimated that degradation of generator performance from this effect would be less than 1%.

Figure 29. Test apparatus used to evaluate the performance of segmented thermoelements as a 4-element module.

Table 5. SUBLIMATION LOSSES OF MCC 60 SPECIMEN 16-1-N MAINTAINED AT ~1200°C AND 10^{-5} - 10^{-6} mm Hg

Time, hr.	Specimen wt., g	Weight Loss g	Weight Loss %	Weight Loss Accumulative, %
0	9.1288			
83.3	9.0601	0.0637	0.70	0.70
193.3	9.0118	0.0483	0.53	1.23
347.8	8.9821	0.0297	0.33	1.56
501.1	8.9616	0.0205	0.29	1.85
655.6	8.9444	0.0172	0.19	2.04
791.6	8.9325	0.0119	0.13	2.17
943.6	8.9205	0.0120	0.13	2.30

Further sublimation loss data n- and p-type MCC 40 specimens are presented in Table 6.

Table 6. SUBLIMATION LOSSES OF MCC 40 SPECIMENS MAINTAINED AT ELEVATED TEMPERATURES AND 10^{-5} - 10^{-6} mm Hg

Test Temperature 850°C, Specimen No. STE-11 PLT (p-type)

Time, hr.	Specimen wt.,g	Weight Loss g	Weight Loss %	Weight Loss Accumulative, %
0	10.8413	-	-	-
20	10.8377	.0036	.033	.033
133	10.8368	.0009	.008	.042
289	10.8359	.0009	.008	.050
444	10.8353	.0006	.006	.055
569	10.8348	.0005	.005	.060
723	10.8344	.0004	.004	.064
879	10.8343	.0001	.001	.065
	Specimen No. Y-3 (n-type)			
0	11.0435*	-	-	-
12	11.0378*	0.0057*	0.05*	0.05*
142	11.0319*	0.0059*	0.05*	0.10*
298	11.0314*	0.0005*	0.01*	0.11*
450	11.0307*	0.0007*	0.01*	0.12*
575	11.0247	0.0060	0.05	0.17
729	11.0230	0.0017	0.02	0.19
851	11.0225	0.0005	0.01	0.20

*Test made at 700°C, rather than 850°C

When after 450 hr at 700°C it was observed that the sublimation loss was quite low for MCC 40 (n-type) the experiment was continued at 850°C. The sublimation loss rate at 850°C was essentially the same as that at 700°C in a vacuum of 10^{-5} - 10^{-6} mm Hg.

In connection with the above sublimation loss data, it is important to note that the MCC 40 materials will be used in the generator at an average temperature well below 850°C, hence losses by sublimation will be well below the above rates. It is not expected that degradation of generator performance from sublimation of MCC 40 materials will exceed 1% in a year's operation of the generator.

Tests were also run for 152 hr at 1200°C in a vacuum of 10^{-5} - 10^{-6} mm Hg, to determine whether beryllia reacts with:

a. columbium (1% Zr) alloy
b. molybdenum-coated columbium alloy

This experiment was deemed necessary since beryllia was to be used to thermally couple the heat source (a sodium potassium liquid metal contained in a 7/16" I.D. pipe) to the hot end of the advanced experimental model generator. No indication of reaction was found.

III. GENERATOR DESIGN

A. THEORETICAL DESIGN OPTIMIZATION

In the design of a thermoelectric generator a multitude of material property and physical size parameters can affect the over-all performance of the generator. Examples of such parameters are:

Material	Physical Size
Seebeck coefficient	Length-to-area ratio
Resistivity	Cross-sectional area
Thermal conductivity	Radiator capabilities
Operating temperature limitations	Spacing around a central core
	Over-all ΔT
	Over-all thermoelement length

Hand calculation methods are available for determination of the maximum efficiency obtainable from a given set of material properties and for the over-all watts/lb ratio for various physical dimensions.

The proximity of MRC to ASD's IBM 7094 computational facilities, enables us to take advantage of machine computation for generator optimization (for example), a hand calculation taking approximately 2-1/2 hr is processed by the IBM 7094 in less than 30 seconds, using the computer program developed on this project.

1. Outline of the Computer Program

The computer program was divided into two main sections: the first determined the optimized efficiency of the couple, and the second determined the optimum watts/lb ratio obtainable with a given physical design.

The efficiency optimization portion was a direct application of a method described by Swanson.(1) The input data include the Seebeck coefficients, resistivities, and thermal conductivities of the individual segment materials, bond resistances, segment interface temperatures (including hot and cold junctions), cross sectional area of the p-leg, and the over-all thermoelement length. From these data are computed the n-leg area, individual segment lengths, internal and optimized load resistances, current and voltage output, and the optimized thermoelectric efficiency.

---

(1) Swanson, B. W., Somers, E. V. and Heikes, R. R., "Optimization of a Sandwiched Type Device," J. Heat Transfer, Transaction of ASME, p-77, Feb 1961.

The watts/lb optimization portion comprises the following steps:

a. From over-all voltages and power requirements the number of couples necessary in series for the voltage and parallel for the current output is calculated.

b. From the physical dimensions given (over-all length, minimum inside diameter and thermoelement spacing), the number of elements in a vertical and horizontal row are determined.

c. The radiator requirement to meet the heat throughput is determined.

d. The weights of the individual components are summed, and the over-all watts/lb ratio obtained.

e. The number of elements in a vertical row is reduced by one and steps b through d are repeated until an optimum watts/lb ratio is achieved.

B. COMPARISON OF THEORETICAL AND EXPERIMENTAL DATA

To bridge the gap between theory and practice the first phase of the optimization procedure required matching the computer calculated results with those obtained by experiment.

The original plan was to use the same 0.5" dia. thermoelement size as in the previously constructed experimental model generator since hot-pressing and junction-forming techniques were perfected for this size. Table 7 shows the agreement between experiment and theory for the 0.5" dia. thermoelements.

As the calculations progressed using these properties for a single couple it became apparent that the over-all weight of the generator based on 0.5" dia. thermoelements would prevent a nominal 10 watts/lb from being achieved. It was therefore necessary to decrease the thermoelement diameter while maintaining the same L/A ratio.

Maintaining the same L/A ratio permits the heat throughput and efficiency to remain the same, providing resistance at the interfaces between various thermoelectric segments and end contacts is negligible. Thermoelements of 0.375" dia. offered attractive weight savings and were amenable to fabrication by hot-pressing. This size thermoelement was chosen and calculations made to check agreement between theoretical and experimental results. Table 8 illustrates this agreement.

Table 7. COMPARISON OF THEORETICAL AND EXPERIMENTAL PERFORMANCE OF 0.5" DIAMETER BY 1" LONG SEGMENTED THERMOELEMENTS AS A p-n COUPLE OPERATING BETWEEN 1200°C AND 460°C

Property		Theoretical*	Experimental
Efficiency		2.92%	-
Power output		0.988 watts	0.970 watts
Current		6.06 amps	6.0 amps
Voltage (load)		0.162 volts	0.162 volts
Resistance		0.0295 ohms	0.0296 ohms
Segment lengths	MCC 50 (p)	1.34 cm	1.2 cm
	MCC 40 (p)	1.06 cm	1.2 cm
	MCC 60 (n)	1.21 cm	1.2 cm
	MCC 40 (n)	1.19 cm	1.2 cm
Effective Seebeck coefficient		436×10^{-6} volts/°C	433×10^{-6} volts/°C

* Computer calculated results obtained by adjusting the Seebeck coefficients and contact resistances.

Table 8. COMPARISON OF THEORETICAL AND EXPERIMENTAL PERFORMANCE OF 0.375" DIAMETER BY 0.65" LONG SEGMENTED THERMOELEMENTS AS p-n COUPLE OPERATING BETWEEN 1200°C AND 460°C

Property		Theoretical*	Experimental
Efficiency		2.8%	-
Power output		.550 watts	0.554 watts
Current		3.50 amps	3.52 amps
Voltage (load)		.157 volts	0.156 volts
Resistance		.0395 ohms	0.0395 ohms
Segment lengths	MCC 50	.62 cm	0.71 cm
	MCC 40 (p)	1.03 cm	0.94 mc
	MCC 60	1.03 cm	0.71 cm
	MCC 40 (n)	.62 cm	0.94 cm
Effective Seebeck coefficient		419×10^{-6} volts/°C	425×10^{-6} volts/°C

* Computer calculated results obtained by adjusting the Seebeck coefficients and contact resistances.

To obtain agreement between the theoretical calculations and experimental values, presented in Tables 7 and 8, it was necessary to use Seebeck coefficients lower than those reported in Figure 2. The reasons for the lower Seebeck coefficient obtained experimentally when the individual materials are joined to form a segmented thermoelement are not yet understood. The lower experimental power output reported in Table 8 for the couples based on 0.375" dia. thermoelements, as compared with that for the 0.5" dia. couple in Table 7, resulted from higher contact resistance.

C. DESIGN OPTIMIZATION

A series of calculations was made for each of the thermoelement diameters to study the effect of length and cold junction temperature on the over-all watts/lb ratio. It was immediately apparent that the limiting design factor was the cold junction radiator area.

The calculations concerned with 0.5" dia. thermoelements used a total radiator area equal to the outer cylindrical surface of the generator itself. This size radiator imposed a severe limitation on the generator performance as it was impossible to radiate sufficient heat at temperatures below 600°C. By adding 1 inch long fins to this configuration, the total radiator area was increased to the extent that the cold junction temperature should remain below 500°C. Such fins also served to strengthen the thin radiators.

The results of the optimization calculations are shown in Figure 30 where the effect of cold junction temperature and over-all thermoelement length on the generator watts/lb ratio for the hot-end temperature of 1200°C may be seen. The final optimized design was the result of several trade-offs between cold-end heat radiation and segment lengths. At a fixed cold-end temperature, the heat transferred through an individual thermoelement is inversely proportional to its length. Thus, increaseing the length would reduce the radiator area requirements. Conversely, though, the power output of the element is reduced and its weight is increased.

At a fixed thermoelement length, a low cold-end temperature would be advantageous from the standpoint of power output. This is counteracted, however, by the larger radiator area required (and the larger over-all generator size to privide this area).

The resultant optimized design based on 0.375" dia., thermoelements operating between 1200°C-500°C, is summarized in Table 9.

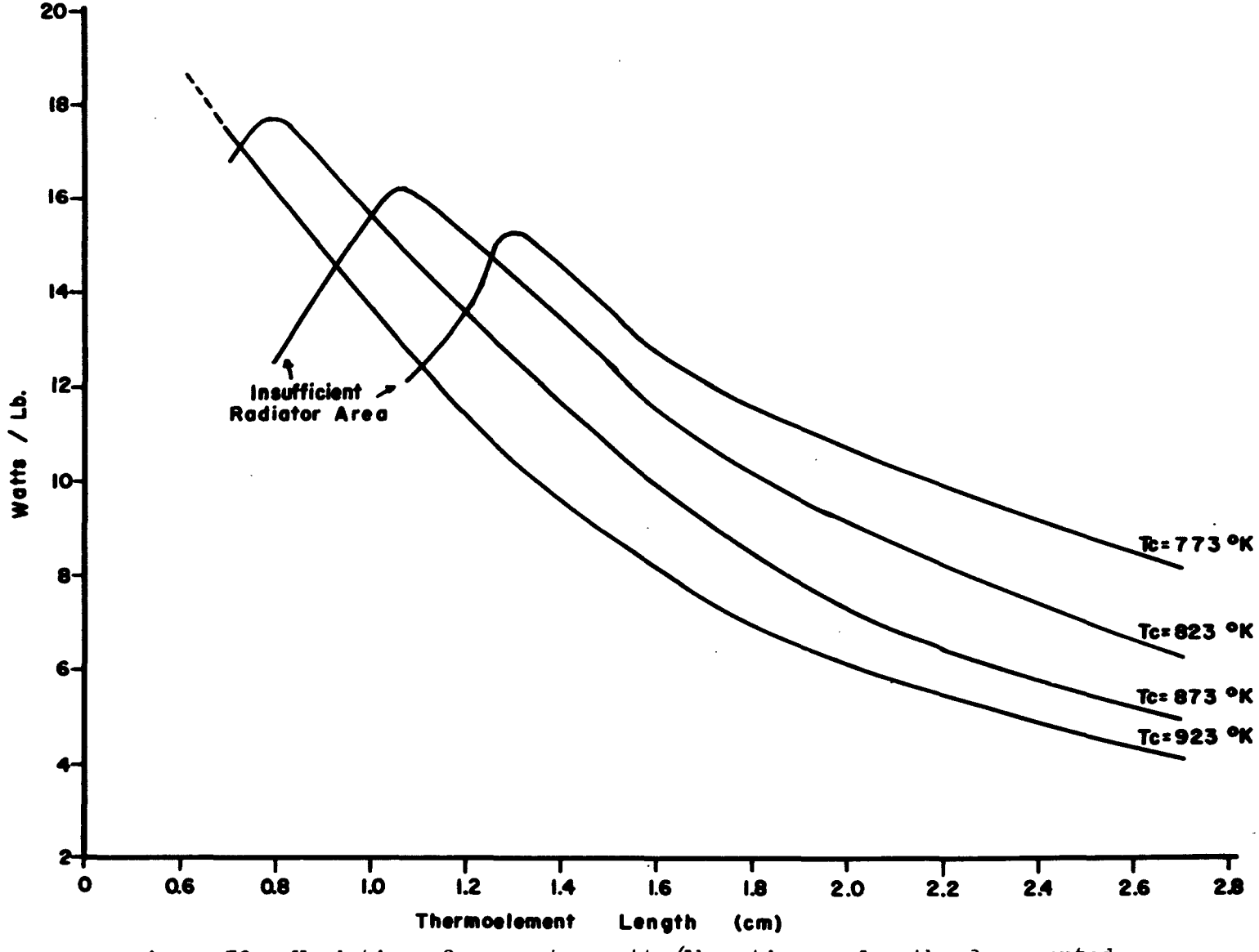

Figure 30. Variation of generator watts/lb ratio vs. length of segmented thermoelements at hot-end temperature of 1200 °C and different

Table 9. OPTIMIZED DESIGN OF ADVANCED EXPERIMENTAL MODEL GENERATOR BASED ON 0.375" DIAMETER THERMOELEMENTS

1200°C Hot end and Cold End Temperature of 500°C

Number of couples in series	46	
Number of couples in parallel	2	
Outside generator dia. (less fins)	8.00 cm	(3.15")
Over-all generator length	31.50 cm	(12.4")
Over-all segment length	1.30 cm	(0.51")
MCC 50 (p)	.491 cm	(.193")
MCC 40 (p)	.809 cm	(.319")
MCC 60 (n)	.815 cm	(.321")
MCC 40 (n)	.485 cm	(.191")

Weight of individual components

p-leg thermoelements (3.8 g. ea.)	350 g.
n-leg thermoelements (4.0 g. ea.)	369 g.
Center core (graphite + BN spacers + BeO packing)	341 g.
Radiators with TEC-1 coating	495 g.
Fiberfrax insulation	110 g.
Electrical leads	30 g.
Total weight	1695 g. 3.74 lb
Total electrical output,	57.3 watts
Watts/lb	15.3
Over-all efficiency	2.5%

The effect of radiator size limitations is clearly indicated in Figure 30. Here, for cold end temperatures of 773, 823, and 873°K, the point at which the 0.01" thick radiator becomes insufficient causes an immediate reduction in the watts/lb ratio. No upper limit has been found for the 923°K case as calculations were not made for thermoelement lengths under 0.7 cm.

The final design shown in Figure 31, does not coincide with that indicated by the optimization calculations. The prime reason for this difference is that fabrication of the very short thermoelements required for optimum watt/lb is not possible at this time.

D. DETAILED DESIGN OF THE ADVANCED EXPERIMENTAL MODEL GENERATOR

Since only cylindrical hot-pressed thermoelements were available, a simple radial design concept was used in which the heat source is centrally located and from which the thermoelements extend radially outward. Its chief advantage is that it allows room for the radiator area needed for rejecting unused thermal energy in a space environment. Additionally, it permits considerable flexibility in physical dimensions and power capacity.

The detailed design of the advanced experimental model generator, submitted herewith for approval by the project engineer, is shown in Figure 31. As shown by the simple electrical circuit at the bottom portion of this figure, the generator would consist of 47 series-connected stages of doubly (parallel)-connected 0.375" dia. by 0.65" long p- and n-type segmented couples. These thermoelements would be joined at their hot ends by molybdenum-graphite contacts and at their cold ends by finned copper radiators coated with TEC-1. This generator design will produce 50-watts at 6 volts (nominal) and weighs an estimated 4.09 pounds. Thus, the nominal output should exceed 10 watts/lb, excluding heat source.

The important individual components of this design are listed in Table 10.

This generator design can be modified to accommodate a heat source supplied by a liquid metal loop, a nuclear isotope source or a concentrated solar energy beam. Various methods for maintaining the rings of thermoelements in their proper position can be provided, depending on the type and physical shape of the prime heat source. On the basis of Air Force plans to test this unit with an electrical heat source, an insulated external hold-down probe (not shown) applying pressure between the bottom plate (item 4) and the top plate (item 5) will be used. For an isotope heat source, a threaded stud could be provided at each end of a ceramic-coated metal isotope container to permit holding the generator structure together. To provide for a nuclear heated liquid metal heat source, metal plates at each end of the generator could be loaded by means of an external spring system or pressure loaded bellows system and fitted around piping from the liquid metal loop.

The design and fabrication of a thermoelectric generator of higher watts/lb ratios and greater efficiency for use in space with the present thermoelectric materials will depend on learning how to make thermoelements of smaller diameters and on further improvements of merit factors for thermoelectric materials.

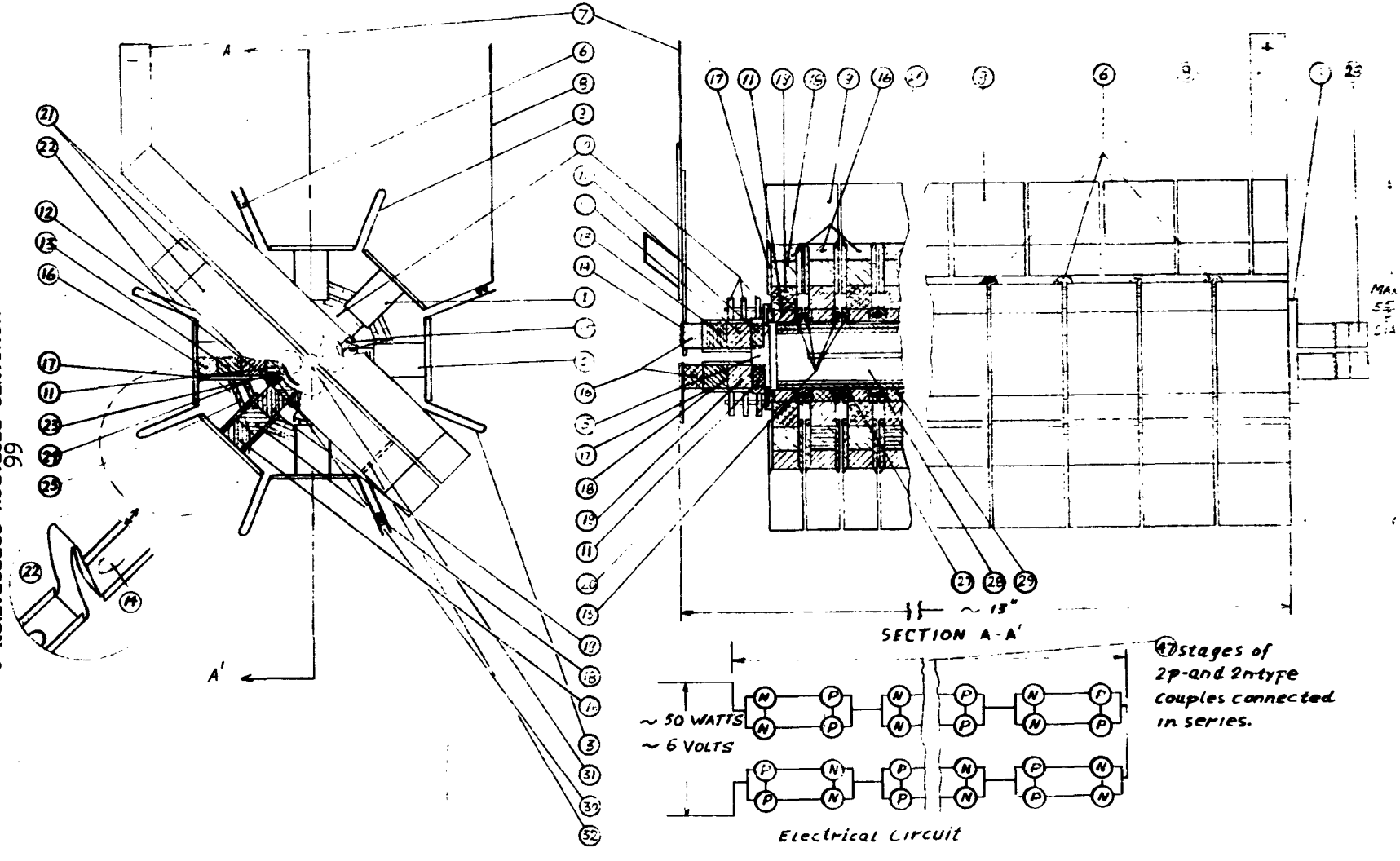

Figure 31. Assembly drawing of the advanced experimental model generator.

Table 10. DESCRIPTIVE LIST OF COMPONENTS AND ESTIMATE OF WEIGHT FOR THE ADVANCED EXPERIMENTAL MODEL GENERATOR*

Component	Description	No. Req'd.	Wt., each, g.	Total wt.,g.
1	0.375" dia. segmented p-type thermoelement	94	4.86	456.8
2	0.375" dia. segmented n-type thermoelement	94	5.03	472.8
3	0.01" thick copper radiator, providing ~1 sq. in. area/ thermoelement	11	11.27	124.0
4	Bottom boron nitride plate	1	3.00	3.0
5	Top graphite plate	1	5.00	5.0
6	Spacer for electrical insulation	69	0.3	20.7
7	0.01" thick upper radiator with negative current lead out	1	10.30	10.3
8	Positive current lead out and 0.01" thick radiator connecting two thermoelectric elements	1	8.49	8.4
9	0.01" copper radiator connecting 4 thermoelelectric elements	11	11.27	124.0
10	Molybdenum radiation shields	3	1.65	5.0
11	Hot end of thermoelectric element (graphite)	-	-	-
12	High temperature thermoelectric element, n-type MCC 60	-	-	-
13	Low temperature thermoelectric element, n-type MCC 40	1	-	-
14	Flame-sprayed copper connection on cold end	188	0.4	75.2
15	Split graphite ring	23	5.20	119.6

* Based on design presented in Figure 31

Table 10(Cont'd)

Component	Description	No. Req'd	Wt., each. g.	Total wt., g.
16	Cold end of thermoelectric element (graphite)	-	-	-
17	Fiberfrax insulation sleeve	188	0.11	20.6
18	Low temperature thermoelectric element, p-type MCC 40	-	-	-
19	High temperature thermoelectric element, p-type MCC 50	-	-	-
20	Boron nitride spacers for electrical insulation	1	2.5	2.5
21	0.01"copper radiator connecting top two thermoelectric elements	1	7.20	7.2
22	0.01 $in.^2$ copper radiator connecting 4 thermoelectric elements	23	11.27	259.2
23	Flame sprayed moly-alumina	23	2.0	46.0
24	First radiation shield	8	3.47	27.8
25	Second radiation shield	8	4.60	36.8
26	Boron nitrdie ring for inulation between graphite rings	22	1.14	25.0
27	Thoria tubing, 13' long 27/32" I.D. and 15/16" O.D.	1	281.2	281.2
28	Split tungsten tubing heater, 14" long 27/32" O.D. x 783" I.D.	1	339.3	339.3
29	Beryllia or boron nitride powder to fill space between thoria tubing and graphite rings		30.0	30.0
30	Flame sprayed electrical (beryllia) insulation at each end of the split graphite ring (compound 15)	46	0.1	4.6

Table 10(Cont'd)

Component	Description	No. Req'd	Wt., each g.	Total wt., g.
31	Opening in top radiator for insertion of a hold-down pin	-	-	-
32	Electrical connection from top stage to first 8-thermo-element tier	1	7.10	7.1
Total weight including heater components 27, 28 and 29.				2512.1 g. (5.52 lb)
Weight of heater components 27, 28 and 29				640.5 g. (1.43 lb)
Total generator weight excluding heater components				1861.6 g. (4.09 lb)

E. THREE-TIER SUBASSEMBLY

While completing design details for the advanced experimental model, a prototype 3-tier 24-thermoelement subassembly, complete with radiators, was fabricated and studied to uncover design, fabrication, and operating problem areas. The initial unit was fabricated from six 4-thermoelement sections like that shown in Figure 32. Each such section consisted of four 0.5" dia. segmented p- and n-type thermoelements joined at their hot ends to a graphite half-circle, in accordance with the detailed design presented in the preceding section.

The initial 3-tier prototype subassembly is shown partially disassembled in Figure 33 after exposure of 200 hr to temperature that reached 1250°C. This subassembly, because of its small 0.5 sq. in./thermoelement radiator area and the crudely installed thermal insulation between vertical rows of thermoelements, experienced ΔT's of less than 630°C and produced only 4.85 watts. Its main function was to demonstrate that the thin radiators must be strengthened to prevent warping and to substantially increase radiator area per thermoelement, so as to obtain higher ΔT's and power output. The warping problem was so sever that strong metallurgical bonds between the copper radiator and the cold ends of the thermoelements were ruptured, causing loss of power output. To minimize warping, edges of the radiators on the end-product generator (see Figure 31) will be turned up to form channels.

It is planned to produce a new 3-tier subassembly using segmented 0.375" dia. thermoelements and with finned radiators providing at least 1 sq. in. of area per thermoelement. Tests will be run on this unit while fabricating the remainder of components required for the advanced experimental generator.

Figure 32. Four-element section of 2 p- and 2 n-type segmented thermoelements connected at their hot ends by a graphite shoe.

Figure 33. Initial 3-tier subassembly constructed with 12 each segmented p- and n-type thermoelements, each 0.5 " diameter by ~ 1" long.

IV. CONCLUSIONS

Based on results of the disassembly and inspection of the experimental 5-watt model generator after 2556 hr sustained performance testing at 1200°C in a vacuum, it is concluded that:

1. The p-type MCC 50 thermoelements were not visibly affected by the prolonged test.

2. A major factor contributing to the approximate 10% change in generator power output, experienced after disassembling and reassembling the generator prior to the sustained performance test, was due to loose contacts between the graphite and molybdenum wire at the hot end junctions of the generator.

3. Direct exposure to the high temperature of the heat source caused failure of the inner layer of molybdenum radiator shields and exerted a harmful affect on the generator output and efficiency. This problem can be minimized.

4. Evaporation of resistance heater materials may have caused partial electrical shorting between some of the series-connected 3-thermoelement generator sections. Protection aginst this problem, which affects voltage output, can be provided.

On the basis of the properties of the four standardized thermoelectric materials and the high emissivity of the TEC-1 radiator coating determined this quarter, it will be possible to build a generator of ~10 watts/lb performance. Providing future progress is made in overcoming problems concerned with producing (by hot-pressing and plasma-spraying techniques) smaller segmented thermoelements of these and improved standardized materials, generators capable of power/weight ratios above 20 watts/lb appear feasible.

V. FUTURE PLANS

Effort during the next quarter will be devoted to fabricating the advanced experimental model generator. Additionally, further sustained testing on a p-n couple of the standardized thermoelectric materials will be conducted and an evaluation of representative MCC 50 thermoelements from the experimental 5-watt model generator will be attempted to permit a direct comparison of their thermoelectric properties before and after the sustained performance test.